Taylor Flow in Microchannels: A Review of Experimental and Computational Work

R. Gupta, D.F. Fletcher and B.S. Haynes
School of Chemical and Biomolecular Engineering
The University of Sydney,
NSW 2006, Australia
e-mail: david.fletcher@sydney.edu.au

Received: 2 February 2010, Accepted: 3 March 2010

Abstract
Over the past few decades an enormous interest in two-phase flow in microchannels has developed because of their application in a wide range of new technologies, ranging from lab-on-a-chip devices used in medical and pharmaceutical applications to micro-structured process equipment used in many modern chemical plants. Taylor flow, in which gas bubbles are surrounded by a liquid film and separated by liquid plugs, is the most common flow regime encountered in such applications. This review introduces the important attributes of two phase flow in microchannels and then focuses on the Taylor flow regime. The existing knowledge from both experimental and computational studies is presented. Finally, perspectives for future work are suggested.

1. INTRODUCTION

The flow in micro-structured devices can be single phase gas or liquid flow or a multiphase flow, i.e. a combination of different phases, for example gas-liquid, liquid-liquid etc. The dynamics of single phase flow in microchannels is very similar to that in large diameter channels and correlations developed for large channels can be used for micro devices (Herwig and Hausner, 2003; Sharp and Adrian, 2004; Hetsroni *et al*., 2005; Kohl *et al*., 2005; Morini *et al*., 2007; Park and Punch, 2008) for channel sizes that are sufficiently large that no new physics is introduced. However, this is not the case for multiphase flow and therefore a lot of effort has gone into understanding multiphase flow in microchannels over the last few decades. In this review, the Taylor regime is examined, from both experimental and modelling perspectives. Its importance amongst the various flow regimes is explained later in this paper.

This review article is laid out as follows: Section 2 describes the important characteristics of two-phase flow in microchannels. Section 3 describes some of the remaining issues in the understanding of two-phase flow. Section 4 presents reviews existing experimental and computational work on Taylor flow. Section 5 gives a brief discussion of the available approaches by which information on Taylor flow can be obtained. A detailed description of conservation equations and numerical techniques in use is presented and Section 6 presents some conclusions and perspectives for future work.

2. FUNDAMENTALS OF MULTIPHASE FLOW IN MICROCHANNELS

As the channel dimensions decrease, some effects which are not important in large diameter channels become dominant. In this review, multiphase flow in millimetre-size channels is studied. The relative importance of different forces is examined by introducing the relevant non-dimensional numbers governing multiphase flow and then the effect of the channel size on the flow physics is discussed.

2.1. Relative Importance of Different Forces

Depending upon the interaction amongst the gravitational, interfacial, inertial and viscous forces, the multiphase flow in microchannels can take different forms, such as suspended droplets, channel-spanning slugs and annular flow. The relative importance of these forces can be understood using the non-dimensional numbers listed in Table 1. Several velocity and length-scales may be

Table 1. Important non-dimensional numbers that characterise multiphase flow in microchannels

Name	Formula	Physical Interpretation
Reynolds number	$\frac{\rho v d}{\mu}$	$\frac{\text{Inertial force}}{\text{Viscous force}}$
Froude number	$\frac{\rho v^2}{\Delta\rho g d}$	$\frac{\text{Inertial force}}{\text{Gravitational force}}$
Bond/ Eötvös number	$\frac{\Delta\rho d^2 g}{\sigma}$	$\frac{\text{Gravitational force}}{\text{Surface tension force}}$
Capillary number	$\frac{\mu v}{\sigma}$	$\frac{\text{Viscous force}}{\text{Surface tension force}}$
Weber number	$\frac{\rho v^2 d}{\sigma}$	$\frac{\text{Inertial force}}{\text{Surface tension force}}$

present in different multiphase flow patterns and therefore, the characteristic velocity and length-scales which are relevant to a particular problem in non-dimensional numbers must be chosen correctly. For example, in bubbly flow the length-scale for the gas phase is the average diameter of the gas bubbles. In slug flow, the bubble velocity and mixture velocity are the two characteristic velocities. As the bubble velocity is not known *a priori*, the mixture velocity can be used as a characteristic velocity (Suo and Griffith, 1964).

The Reynolds number is the ratio of inertial and viscous forces. For a channel of 1 mm in diameter and a velocity of 1 m s^{-1}, the Reynolds number for water flow is ~1000. The flow in a smooth duct is laminar below a Reynolds number of ~2300 and becomes fully turbulent around a Reynolds number of 10,000 (White, 1991). This indicates that the flow is generally laminar in microchannels and viscous forces remain significant, especially at low velocities. For two-phase gas-liquid flow, there can be different definitions of the Reynolds number depending upon the flow rates and physical properties of the two phases. The appropriate definition of the Reynolds number depends upon the flow pattern and the particular flow regime for which it is to be used.

In almost all of the flow patterns observed in two-phase gas-liquid flow in microchannels, a liquid film is present at the wall, where viscous forces are important. Therefore, it is meaningful to use properties of the liquid in the definition of Reynolds number. When the gas and liquid superficial velocities are of the same order, the inertia of the gas phase is negligible compared with that of the liquid and only the liquid Reynolds number is important. When the gas superficial velocity is high relative to the liquid superficial velocity (for example in annular flow), the inertia of the gas can become important and both the liquid and gas phase Reynolds numbers are important in characterising the flow. In slug and annular flows, where a liquid film exists at the wall, the liquid film thickness is an important length-scale and therefore the film Reynolds number is an important parameter in describing the film flow characteristics.

The Froude number compares the inertial force with the buoyancy force. For gas-liquid flow in a channel of 1 mm diameter, the Froude numbers are 0.01, 1 and 100 for characteristic velocities of 0.01, 0.1 and 1 m s^{-1}, respectively. This suggests that the gravitational force could play an important role in some flow conditions in millimetre-size channels.

The Bond number is the ratio of the gravitational and surface tension forces. For air-water flow in a channel of 1 mm diameter, the Bond number is 0.14. Since the Bond number depends on the second power of the diameter, the importance of gravity diminishes quickly as the channel diameter is reduced. In fact, this is the reason why stratified flow is not observed in gas-liquid flow in microchannels. Barnea *et al*. (1983) derived a critical Bond number at which stratified flow changes to slug flow by applying a force balance between the surface-tension and gravitational forces, as given in eqn (1). For gas-liquid flow ($\rho_G << \rho_L$), the critical Bond number is 4.7, calculated using eqn (1) below.

$$Bo_{crit} = \frac{(\rho_L - \rho_G)d^2 g}{\sigma} = \frac{1}{\frac{\rho_L}{\rho_L - \rho_G} - \frac{\pi}{4}} \quad (1)$$

The Capillary number is the ratio of the viscous and surface tension forces and is an important parameter in two-phase flow in microchannels. For air-water flow and a mixture velocity of 1 m s^{-1}, the Capillary number is 0.014. For very viscous fluids, such as silicon oil, the Capillary number becomes higher (~O(1)). Another important point to note here is that the Capillary number does not contain any length-scale information and is the ratio of two forces which both increase in importance with decreasing channel size.

The Weber number is the ratio of the inertial and surface tension forces and can also be written as the product of the Reynolds and Capillary numbers ($We = Re\ Ca$). As will be explained later, the Weber number provides a better characterisation than the Reynolds number when inertial forces are important.

The last three non-dimensional groups in the Table 1, the Bond, Capillary and Weber number compare the surface tension force with the gravitational, viscous and inertial forces, respectively. These groups indicate that as the channel size (and velocity) decreases, the surface tension force becomes more important.

2.2. Size Effects

A reduction in the channel size gives rise to certain physical phenomena that are not significant in large diameter channels but become important with a reduction of the channel size. This section discusses such effects.

2.2.1. Surface-to-Volume Ratio

The large surface-to-volume ratio, or specific surface area, is an important characteristic of microchannels and is inversely proportional to the length-scale of the channel cross-section. The large surface area-to-volume ratio leads to high rates of heat and mass transfer, making the use of micro-structured devices as heat exchangers, mixers and reactors appealing. The increased specific surface area can also be utilised in catalytic gas phase reactors coated with the active material on the inner wall.

2.2.2. Surface Forces

The type of forces (body or surface) that govern the physical phenomena in a channel depends upon the length-scale. Body forces are scaled with the third power of the length-scale while surface forces depend on the first (for example surface tension and viscous forces) or second power of the length-scale. Therefore, below a certain length-scale, surface forces are dominant compared with body forces (Ho and Tai, 1998). Some examples of surface forces in multiphase flow in microchannels are surface tension, frictional (viscous) force and wall adhesion etc.

2.2.3. Wall Wettability

Wall wettability is another important surface effect that can become significant in multiphase flow in microchannels. In continuum models, the three-phase contact angle, i.e. the angle between the solid wall and gas-liquid interface in contact with it, is used to measure wettability of a liquid on a solid wall. The static three-phase contact angle is a result of the balance among the adhesive (attraction force between liquid and solid wall, liquid and gas molecules) and cohesive (attraction force among liquid molecules) forces. When the contact line moves, the contact angle does not remain constant and the complex phenomena of contact angle dynamics need to be accounted for (for example, see (Mourik *et al*., 2005; Ajaev and Homsy, 2006; Afkhami *et al*., 2009)). This review deals with Taylor flow, for which the walls are covered by a liquid film, and therefore this effect is unimportant, except possibly in the mixing region where the gas and liquid are brought into contact.

2.2.4. Laminar Flow

In microchannels the Reynolds numbers are relatively low so that laminar flow is much more common than turbulent flow. The fundamental equations of flow, heat and mass transfer can be solved

directly without reference to any heuristic models, such as those required to model the effects of turbulence. This allows, in theory, the prediction of transport phenomena to be made more accurately in microchannels than in large channels, where the flow is generally turbulent. However, this laminar nature of the flow often gives rise to the need for additional means of mixing to achieve high transport or reaction rates. The use of obstacles on the channel wall (Stroock *et al*., 2002), varying channel cross-sections (Hardt *et al*., 2003) and having tortuous channel paths giving rise to secondary flow helps to enhance mixing at low Reynolds numbers. The Dean vortices (observed in transverse plane) generated by centrifugal forces in tortuous channels can enhance the rate of heat transfer significantly without a corresponding rise in the pressure drop (Gupta *et al*., 2008). Slug flow occurring in gas-liquid and liquid-liquid flows also gives rise to high transport rates (Günther *et al*., 2004).

2.2.5. Continuum Hypothesis

For flow in millimetre-size channels the channel dimension is significantly larger than the molecular mean free path (O (10^{-8}) m for gas). As a result the Knudsen number (the ratio of molecular mean free path and a characteristic dimension of the flow) is very small and consequently the continuum assumption applies. The liquid film surrounding a gas bubble can be of the order of a few microns. The assumption of continuum behaviour in the thin liquid films (O (10^{-6} m)) is also usually valid. However, molecular forces, such as Van der Waals forces, can be important for ultra thin liquid films.

Other effects of channel size reduction, such as the formation of an electric double layer (EDL) (Bayraktar and Pidugu, 2006), slip at the channel wall (Thompson and Troian, 1997; Craig *et al*., 2001), viscous energy dissipation (Koo and Kleinstreuer, 2004) are not considered here because we are concerned with relatively large (order of millimetres) sized channels where these effects are negligible and therefore they are not discussed further.

3. OPEN RESEARCH QUESTIONS IN GAS-LIQUID TWO-PHASE FLOW

Despite the large and ever increasing effort deployed in the study of multiphase flow in micro-channels there still remain many open questions. These are presented and discussed in the following sections.

3.1. Identification of the Flow Regime Map

The distribution of the gas and liquid phases, and their interaction, determines the behaviour of two-phase flow in a channel. The phase distribution is commonly called the flow pattern or flow regime. The determination of the flow regime map for a given channel is generally the first step in characterising two-phase flow behaviour because it strongly influences the critical thermohydraulic properties, such as pressure drop and the heat transfer rate. The various flow configurations that occur are dependent on the relative gas and liquid properties, flow rates and channel geometry.

Two-phase flow regimes in microchannels have been experimentally investigated by Suo and Griffith (1964), Barnea *et al*. (1983), Damianides and Westwater (1988), Barajas and Panton (1993), Fukano *et al*. (1993; 2007), Mishima and Hibiki (1993; 1996), Tripplet *et al*. (1999a), Coleman and Garimella (1999), Bao *et al*. (1994; 2000), Zhao and Bi (2001a), Chen *et al*. (2002), Pehlivan *et al*. (2006), Saisorn and Wongwises (2008) and Pohorecki *et al*. (2008) amongst others. Although the flow patterns occurring in microchannels are similar to those that occur in large diameter channels, with the exception of the absence of stratified flow, there are certain differences in the flow characteristics in the two. For example, the flow is generally laminar in microchannels unlike in macro-channels. Also, the liquid plug in slug or Taylor flow does not contain bubbles. It is not surprising therefore that flow regime maps used for large channels compare poorly with microchannel data (Akbar et al., 2003).

Figure 1 shows the flow regime map of Triplett *et al*. (1999a) which was developed for air-water two-phase flow behaviour in a horizontal circular channel of 1.45 mm inner diameter in gas superficial velocity (U_G) versus liquid superficial velocity (U_L) coordinates. Five main flow regimes were identified: bubbly, slug, churn, slug-annular and annular. Figure 2 shows the morphology of the representative flow regimes.

At high liquid and low gas flow rates, small gas bubbles are distributed in the continuous liquid phase. At low gas and liquid flow rates, regular periodic bubbles almost filling the channel and

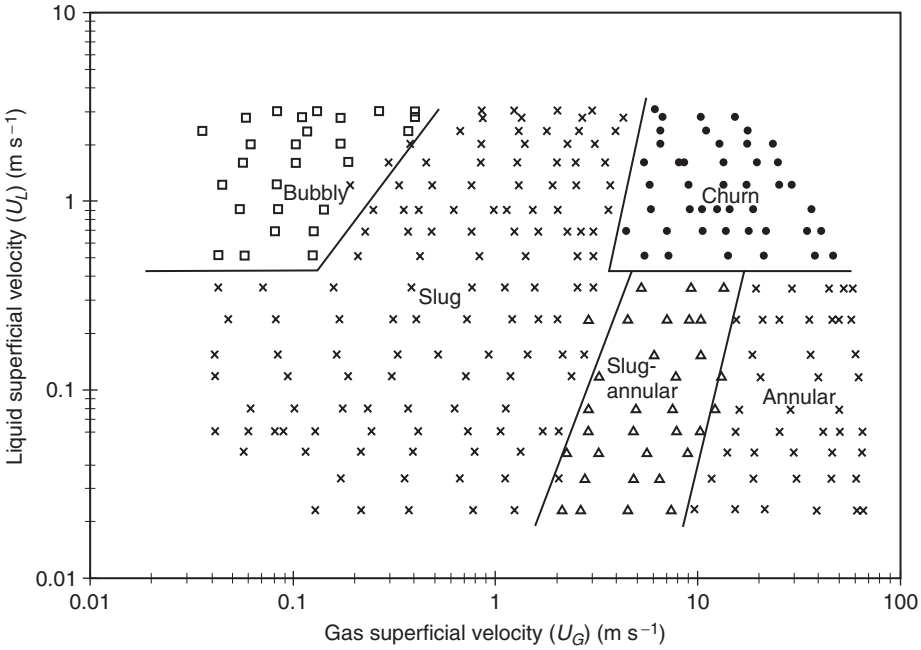

Figure 1. Flow pattern map as observed by Triplett *et al.* (1999a) for a 1.45 mm diameter circular test section. The transition lines are only indicative and are not from Triplett *et al.* (1999).

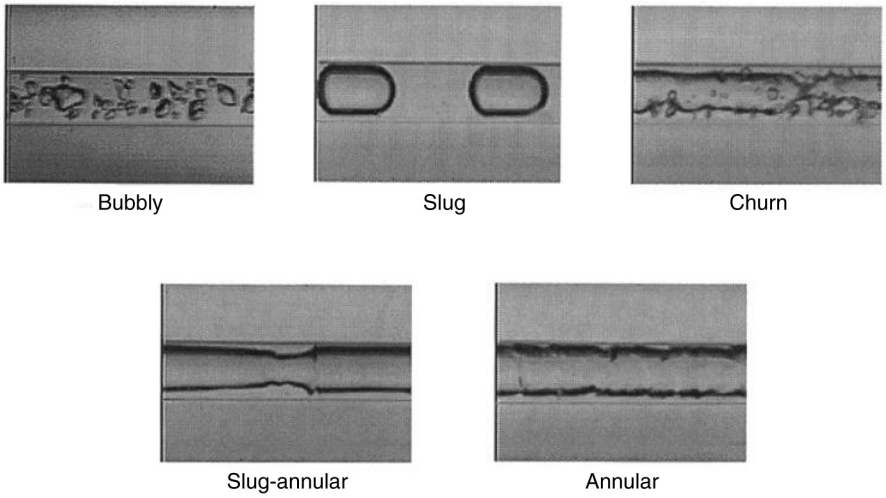

Figure 2. Representative flow patterns of air-water flow in a circular tube of 1 mm diameter as observed by Triplett *et al.* (1999a).

surrounded by a thin liquid film are obtained. Two consecutive bubbles are separated by a liquid slug and the flow pattern is called slug or Taylor flow. As the gas flow rate is increased, the bubbles become longer. An increase in the gas flow rate results in bubble coalescence, so that the gas flows as a continuous core and the gas-liquid interface has large-amplitude waves on it. This flow pattern is called wavy annular or slug annular flow. A further increase in the gas velocity gives rise to annular flow with only small amplitude waves present on the gas-liquid interface. Triplett *et al.* (1999a) identified two mechanisms that lead to churn flow. In one process, the elongated bubbles associated with the slug flow pattern become unstable as the gas flow rate is increased and their trailing ends are disrupted into dispersed bubbles. In another process, the occurrence of churning waves periodically disrupts an otherwise apparently wavy-annular flow pattern.

These major flow regimes are generally in good agreement with those reported by other

researchers (Yang and Shieh, 2001; Chen *et al*., 2002; Chung and Kawaji, 2004; Pehlivan *et al*., 2006; Ide *et al*., 2007), with discrepancies generally due to different descriptions of the various regimes. Shao *et al*. (2009) carried out a detailed review of the boundaries of flow patterns during gas-liquid two-phase flow in microchannels under different flow conditions. They mentioned the occurrence of dispersed flow at high gas and liquid flow rates in which the liquid is dispersed in the continuous gas as droplets with a small liquid film present at the wall. They also pointed out that this flow pattern is not observed very often in microchannels because of the very high gas and liquid velocities required to generate it.

3.2. Pressure Drop and Void Fraction

Another major area of research in gas-liquid two-phase flow in microchannels is the measurement of pressure drop and void fraction. Again much work has been aimed at determining the applicability of correlations developed for macro-channels to microchannels.

Pressure drop is amongst the most important parameters needed for the design of process equipment. However, two-phase frictional pressure drop in microchannels is not well understood despite a number of experimental studies (Fukano and Kariyasaki, 1993; Bao *et al*., 1994; Mishima and Hibiki, 1996; Triplett *et al*., 1999b; Bao *et al*., 2000; Zhao and Bi, 2001b; Dutkowski, 2010). The experimental data have been compared with the existing two-phase pressure drop correlations for large channels, such as the homogeneous flow model (the two phase are assumed to be well mixed and move with identical velocities everywhere) (McAdams *et al*., 1942; Dukler *et al*., 1964; Beattie and Whalley, 1982), and several separated flow models, for example, the Lockhart-Martinelli correlation (Lockhart and Martinelli, 1949), Chisholm (Chisholm, 1967) or Friedel correlation (Friedel, 1979).

While some researchers (Triplett *et al*., 1999b; Bao *et al*., 2000; Pehlivan *et al*., 2006) found that the homogeneous model predicted their data well, others (Zhao and Bi, 2001b; Kawahara *et al*., 2002) suggested that the separated flow model of Lockhart-Martinelli can predict the two-phase flow frictional pressure drop better. Therefore, there is no general agreement about the validity of large-channel correlations for microchannels. Moreover, in most of these studies the original correlations have been modified to fit the data and these modified correlations may be valid only for the specific conditions studied.

All the correlations mentioned above do not explicitly account for the flow pattern and have been developed to cover various flow patterns. Bao *et al*. (2000) observed that the frictional pressure drop is flow regime dependent. Triplett *et al*. (1999b) found that the homogeneous flow model, as well as other widely used empirical correlations for inter-phase slip and wall friction, do not predict the frictional pressure drop in annular flow.

The void fraction is a measure of the percentage of the flow domain occupied by the gas phase during gas-liquid two-phase flow in a channel. The measurement of void fraction in micro passages is quite challenging (Chung and Kawaji, 2004). Most of the experimental data on void fraction in microchannels have been gathered through visualisation and conduction techniques. Similar to those for pressure drop, the correlations used to model the void fraction in microchannels have largely been extrapolated from macroscale models, such as Lockhart-Martinelli (Lockhart and Martinelli, 1949), CISE correlation (Premoli *et al*., 1970) and Armand correlation (Armand and Treschev, 1946; Armand, 1959). Bao *et al*. (1994) found their data to be in good agreement with the Lockhart-Martinelli and the CISE correlations, while Triplett *et al*. (1999b) found that their data were best fitted by a homogeneous mixture assumption. Serizawa *et al*. (2002) obtained good agreement with the Armand correlation in the slug flow regime, while Kawahara *et al*. (2002) did not obtain good agreement with the Armand correlation.

Homogeneous flow models are useful when the gas and liquid are relatively well mixed, for example, bubbly flow. When the gas and liquid phases are separated (slug, slug-annular and annular flow), the pressure drop and void fraction are dependent on the flow pattern. For example, at low flow rates the gas is subjected to very low shear forces (slug flow regime) while the shearing force of the gas is significant at high gas flow rates (annular flow regime) (Inada *et al*., 2004). Such differences in the momentum transfer mechanisms occurring for different flow regimes give rise to flow pattern dependant pressure drop. Most of the available separated flow models for large channels do not include surface tension effects which are important in small channels. Therefore, it is imperative to study the hydrodynamics in these flow patterns.

3.3. Heat Transfer

The mechanisms of heat transfer in microchannels can be divided into two major categories: (i) heat transfer without any phase change and (ii) heat transfer with phase change, i.e. evaporation, boiling and condensation. It is now known that the flow pattern occurring in adiabatic two-phase flow also occurs in two-phase boiling (Chen and Garimella, 2006) and condensation (Chen *et al*., 2008). While there has been a lot of research into understanding the complex phenomena of boiling (Bertsch *et al*., 2008) and condensation (Baird *et al*., 2003; Chen *et al*., 2008), the area of two-phase heat transfer without phase change has been almost completely neglected, despite its importance in understanding the heat transfer mechanisms in boiling and condensation phenomena. For example, an understanding of heat transfer in the annular flow regime would be helpful in the study of boiling and condensation, since even at a quality of 0.2 the flow regime is frequently annular.

3.4. Mass Transfer

The knowledge of flow morphology and hydrodynamics is required for the design of microreactors for given flow conditions and reactants. For example, axial dispersion can be minimised (Pedersen and Horvath, 1981; Trachsel *et al*., 2005) and radial mixing can be enhanced (Horvath *et al*., 1973) in the slug flow regime. Non-catalytic gas-liquid reactions, such as direct fluorinations, have been performed for slug-annular and annular flow conditions (Mas *et al*., 2003). As a result, mass transfer and reaction engineering in multiphase flow in microchannels is studied for specific flow patterns (Kreutzer *et al*., 2005a).

3.5. Detailed Study of Flow Patterns

As explained in the previous sections, understanding the details of the flow characteristics of different flow regimes can help in better predicting the transport rates of heat, mass and momentum. Therefore, in this article, the hydrodynamics and heat transfer in flow regimes where the gas and liquid phase are separated by a well-defined interface (slug, slug-annular and annular flow) are studied. These flow regimes cover a large area of the flow regime map and occur in many industrial applications.

4. SLUG OR TAYLOR FLOW

The slug flow regime covers a wide range of flow conditions for gas-liquid two-phase flow in microchannels. Slug flow also occurs in liquid-liquid flow where a continuous phase of liquid is

Table 2. Industrial applications of slug or Taylor flow in microchannels

Industrial Application	Application
Flow measurement	Measurement of liquid flow velocity (Fairbrother and Stubbs, 1935; Bretherton, 1961)
Chemical processing	Catalyst coating (Kolb and Cerro, 1991), Catalytic reactors: Three phase reactions (Kreutzer *et al*., 2005a), Multiphase reactors (diffusion limited fast reactions): Production of Silica (Khan *et al*., 2004), (Günther *et al*., 2004)
Biomedical	Blood flow in capillaries (Prothero and Burton, 1961), lung airway opening problem (Gaver *et al*., 1996; Suresh and Grotberg, 2005; Zheng *et al*., 2007), gas embolism (Suzuki and Eckmann, 2003), automatic analyser (Begg, 1972; Snyder and Adler, 1976b)
Filtration	Enhancement of microfiltration efficiency (Taha and Cui, 2002; 2004)
Electronics cooling	Cooling of high-density multi-chip modules in supercomputers, high-powered X-ray and other diagnostic devices (Zhao and Bi, 2001).
Heat exchangers	Compact heat exchangers: Printed circuit heat exchangers (Bao *et al*., 1994), high flux heat exchangers in aerospace systems, cryogenic cooling system in satellites.
Fuel cell	Methanol fuel cell (Buie and Santiago, 2009)
Oil and gas industry	Enhanced oil recovery processes (Schwartz *et al*., 1986)

segmented by discrete droplets of the distributed liquid phase (Link *et al*., 2004). Slug flow is known by several other names, such as Taylor flow (after (Taylor, 1961)), plug flow, bolus flow (Prothero and Burton, 1961), segmented flow (Günther *et al*., 2004), intermittent flow and bubble-train flow (Thulasidas *et al*., 1995). As listed in Table 2, Taylor flow is increasingly being used in various industrial processes because of its unique hydrodynamic characteristics. Two adjacent liquid slugs are separated by the gas bubbles and are connected only via a liquid film; this segmentation reduces the axial mixing significantly (Begg, 1971; Snyder and Adler, 1976b; Khan *et al*., 2004). Mass transfer between the two phases is enhanced by internal recirculation within the liquid slug and gas bubble, the large interfacial area and the small diffusion paths. With the increased application of slug flow in various industries, a vast amount of literature is available on transport phenomena in Taylor flow. Recent reviews by Kreutzer *et al*. (2005a) and Angeli and Gavriilidis (2008) provide a good summary of work on Taylor flow in microchannels.

4.1. Film Thickness

In Taylor flow, the gas bubble travels faster than the liquid and a thin film of liquid is left behind. The thickness of this liquid film is important in many applications, such as catalyst coating in monolith reactors (Kolb and Cerro, 1991), heat and mass transfer from the channel wall to the liquid (van Baten and Krishna, 2004; Kreutzer *et al*., 2005a).

Two different classes of methods are found in the literature for estimating the film thickness experimentally: (i) direct methods: the film thickness is directly measured using high quality images either free from the optical distortion caused by curved channel wall (Aussillous and Quéré, 2000) or corrected for the optical distortion (Han and Shikazono, 2009) (ii) indirect methods: the bubble velocity is determined experimentally and then the film thickness is calculated using continuity. This requires knowledge of the velocity profile in the liquid film. While some researchers have treated the film as being stagnant (Suo and Griffith, 1964; Warnier *et al*., 2008), others assumed a fully-developed annular flow velocity profile or fully-developed velocity profile in the liquid film with a no shear boundary condition at the interface (Thulasidas *et al*., 1995).

Bretherton (1961) derived an expression for the liquid film thickness given by eqn (2) using lubrication approximation (film thickness assumed to be very small compared with the channel radius) and neglecting the inertia term ($We = ReCa \ll 1$). The film thickness obtained from Bretherton's correlation agrees well with experimentally measured film thicknesses for $10^{-4} < Ca < 10^{-2}$. However, at Ca values below 10^{-4} and above 10^{-2}, Bretherton's correlation does not agree well with the experimental measurements. Ratulowski and Chang (1990) showed that, by taking into account the surfactant effects, the difference between Bretherton's theory and experimental data for very low Ca (where surface tension forces are dominant) can be explained.

$$\frac{\delta_F}{R} = 1.34\ Ca^{2/3} \tag{2}$$

Using dimensional arguments, Aussillous and Quéré (2000) developed a correlation for the film thickness of the form given in eqn (3), where a, b and c are constants.

$$\frac{\delta_F}{R} = \frac{a\ Ca^{2/3}}{1 + b\ Ca^{2/3} - c\ We} \tag{3}$$

For negligible inertia, $a = 1.34$, $b = 3.34$ and $c = 0$ so that the last term in the denominator disappears. In the limit of small Capillary numbers, this correlation approaches the result from Bretherton's analysis. In the case of non-negligible inertia, Aussillous and Quéré (2000) suggested the form given by eqn (3) for the correlation would apply but did not provide the values of the constants.

Using finite-element based numerical methods, several researchers (Giavedoni and Saita, 1997; 1999; Heil, 2001) showed that the film thickness decreases first slightly on increasing the Reynolds number and then increases monotonically. Using a regular perturbation method, de Ryck (2002) studied the effect of inertia on the liquid film thickness in a semi-infinite bubble at Reynolds numbers up to 1000 and showed that the ratio of Reynolds and Capillary number (Re/Ca) plays an important role in determining the effect of inertia on film thickness. As shown in Figure 3, for a

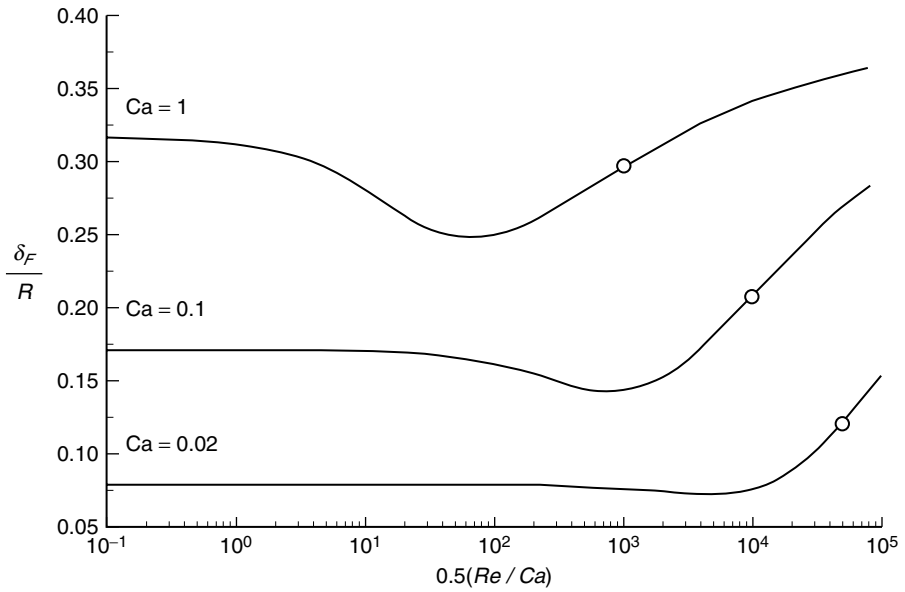

Figure 3. Effect of inertia on the liquid film thickness around the bubble (taken from (de Ryck, 2002)).

particular Capillary number (*Ca*), the fluid inertia does not have any significant effect on the film thickness up to a certain value of Reynolds number (*Re*) beyond which the thickness first decreases slightly and finally increases with an increase in *Re*. The *Re* values above which inertial effects become important decreases with an increase in the Capillary number (*Ca*).

Han and Shikazono (2009) suggested an expression of the form of eqn (4) below for the liquid film thickness at high inertia.

$$\frac{\delta_F}{R} \sim \frac{Ca^{2/3}}{1+Ca^{2/3}+f(\mathrm{Re},\, Ca)-g(We)} \tag{4}$$

Although the terms involving f (*Re*, *Ca*) and g(*We*) in eqn (4) depend on similar variables, they show two contrasting effects of inertia on the liquid film thickness. While, the third term in the denominator, f (*Re*, *Ca*), acts to reduce the liquid film thickness, the last term, g (*We*), contributes to an increase in the liquid film thickness.

In vertical channels, the main effect of gravity is to alter the thickness of the liquid film. If the bubble is travelling upwards, additional liquid accumulates in the film, while in downward flow the liquid film becomes thinner. Bretherton (1961) suggested that the non-dimensional film thickness (δ_F/R) increases by a factor of $\left(1+\frac{1}{6}Bo+O(Bo)^2\right)$ for upward flow and decreases by the factor $\left(1-\frac{1}{6}Bo+O(Bo)^2\right)$ for downward flow. Hazel and Heil (2002) studied the effect of gravity in vertical channels numerically for a Bond number of 0.45 over a range of Capillary numbers and found that the film thickness obtained was not in agreement with Bretherton's correction terms. They also pointed out that the Bond number enters in the governing equations as a dimensionless group of (*Bo*/*Ca*) and so at high values of the Capillary number, the effect of gravity becomes unimportant.

Han and Shikazono (2009) measured the liquid film thickness in horizontal channels at the top, side and bottom of the channel for Bond numbers of about 0.1 and 1.9. For $Bo = 1.9$, significant differences in the liquid film thicknesses at different positions was observed but for $Bo = 0.1$, the film thickness was the same at all the positions.

4.2. Bubble Shape

At low Capillary numbers, the gas bubble can be approximated as a cylinder with hemispherical caps at the ends. For low-viscosity fluids (high value of Re/Ca), the aspect ratio of the nose increases, i.e. the length of the nose increases and the radius of the bubble decreases (de Ryck, 2002). For highly viscous liquids (low value of Re/Ca), this effect is small and there is only a slight change in the aspect ratio. With an increase in the Capillary number, the bubble tail becomes flatter and at still higher values of the Capillary numbers, the bubble tail takes a concave shape (Feng, 2009). This deformation of bubble shape is more prominent at higher Reynolds number (Walsh *et al*., 2009). Near the tail of the bubble, some wiggles are observed in the gas-liquid interface and the amplitude of these wiggles increases with an increase in the Reynolds number (Edvinsson and Irandoust, 1996).

Bretherton (1961) pointed out that the gravitational force can distort the symmetric shape of the bubble at non-negligible Bond numbers. However, he could not obtain the solution of the relevant partial differential equation analytically. Grotberg and co-workers have studied the effect of gravity on the motion of the liquid slug in a planar two-dimensional channel analytically (Suresh and Grotberg, 2005) and numerically (Zheng *et al*., 2007). Suresh and Grotberg (2005) studied the effect of gravity on the motion of a liquid plug in a planar two-dimensional channel by applying lubrication theory in the limit of small Capillary (Ca) and Bond (Bo) numbers. They found that when the gravitational force is small compared with viscous and surface tension forces ($Bo < 1$, $Ca \ll 1$), the film thickness scales as $Ca^{2/3}$; and when the gravitational force is comparable with the viscous and surface tension forces, it scales as $Ca^{1/2}$. They pointed out that in a cylindrical geometry, gravity causes a variation in the film thickness at a cross-section with azimuthal angle. However, the scaling relations obtained for a two-dimensional planar geometry will apply to a cylindrical geometry too.

The length of the liquid slug is an important parameter in predicting the pressure drop, heat and mass transfer in the Taylor flow regime. Several correlations have been proposed to allow calculation of the lengths of the gas bubble and liquid slug, e.g. (Laborie *et al*., 1999; Liu *et al*., 2005; Akbar and Ghiaasiaan, 2006; Qian and Lawal, 2006). These correlations are highly empirical and can predict the data only for a given inlet geometry because the mechanism of bubble break-off is strongly dependent on the inlet geometry and a slight change in this geometry can give rise to very different bubble and slug lengths (Salman *et al*., 2006; Shao *et al*., 2008).

4.3. Flow Field

Taylor (1961) postulated the form of the streamlines in the liquid slug region for different values of the non-dimensional bubble velocity. As shown in Figures 4(a) and (b) for $U_B/U_{TP} < 2$, the central portion of the liquid slug moves with the bubble velocity and this portion shows recirculating motion in a reference frame moving with the bubble. There can be two different kinds of flow pattern possible. As shown in Figure (4a), the stagnation points on the bubble surface form a stagnation ring at the bubble nose. In the other case (shown in Figure (4b)), a stagnation point exists at the bubble tip and a second stagnation point exists in the liquid slug.

In the laboratory frame of reference, the motion in the liquid slug can be decomposed into two components: a forward moving bubble velocity and a recirculating velocity. Thus, the liquid slug is always seen as forward moving in a laboratory frame of reference. As shown in Figure 5, CFD simulations (for example, see (Kreutzer *et al*., 2005a)) and micro-PIV measurements (for example see, (Thulasidas *et al*., 1997; Günther *et al*., 2005)) have confirmed the occurrence of this recirculation motion. Thulasidas *et al*. (1997) also calculated the location of the centre and the size of the recirculating portion of the liquid slug. The second recirculating flow pattern, as shown in Figure (4b) has not been observed experimentally. Taylor also pointed out that for $U_B/U_{TP} > 2$, all the liquid in the slug is left behind and no recirculating motion is observed, as shown in Figure (4c). Such flow is called by-pass flow. Thulasidas *et al*. (1997) observed the occurrence of by-pass flow in their experimental measurements and derived an analytical model to explain the limit of $U_B/U_{TP} = 2$ between circulating and by-pass flow regimes in circular capillaries.

The flow field in the liquid slug in a laboratory reference frame has also been compared with that of liquid-only developing flow (e.g. see (Walsh *et al*., 2009) and references therein). Thulasidas *et al*. (1997) observed that for liquid slugs longer than 1.5 channel diameters, the flow in the liquid slug becomes fully-developed and a parabolic velocity profile is obtained.

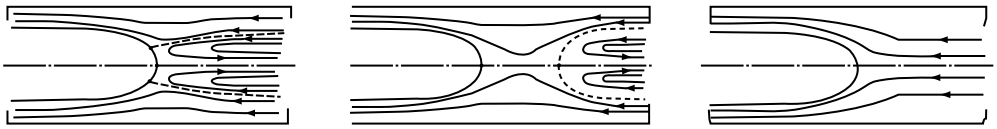

(a) $U_B/U_{TP} < 2$ (b) $U_B/U_{TP} < 2$ (c) $U_B/U_{TP} > 2$

Figure 4. Sketches of possible streamline patterns in the liquid slug (Taylor, 1961) for different values of the bubble velocity relative to the mixture velocity. Cases (a) and (b) differ in the location of the stagnation points: in case (a) they are on the bubble interface and in case (b) one is on the bubble and the other within the liquid slug.

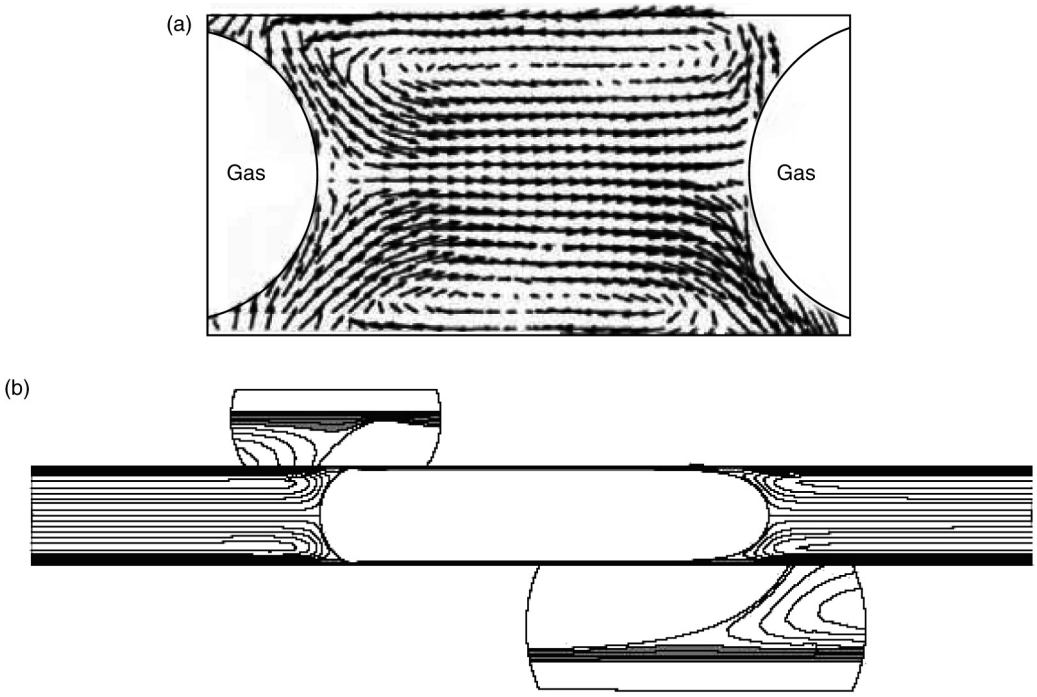

Figure 5. (a) The velocity field in the liquid slug obtained from micro-PIV measurements (the bulk or mixture velocity is subtracted from the streamwise velocity component) (G nther *et al.*, 2005) (b) streamlines in the liquid slug obtained from CFD calculations (Kreutzer *et al.*, 2005a).

Zheng *et al*. (2007) studied the combined effects of gravity, mixture velocity and liquid slug length in a planar two-dimensional, horizontal channel numerically. They pointed out that gravity causes flow of the liquid from the upper liquid film near the nose to the liquid film at the tail of the preceding bubble, as shown in Figure (6). The flow recirculation (in a frame of reference moving with the bubble) becomes weaker with an increase in the Bond number and the number of vortices present in the liquid slug can be zero, one or two depending on the flow parameters. Asymmetry in the liquid distribution (measured as the ratio of liquid volume above and below the centreline of the channel) was found to increase with an increase in Bond and to be reduced by an increase in either of the length or speed of the liquid slug.

4.4. Pressure Drop

The two-phase pressure drop in a unit cell (a gas bubble and two halves of adjacent liquid slugs) can be decomposed into three components (Kreutzer *et al*., 2005b; Han and Shikazono, 2009).

$$\Delta P = \Delta P_{Slug} + \Delta P_{Film} + \Delta P_{Cap} \tag{5}$$

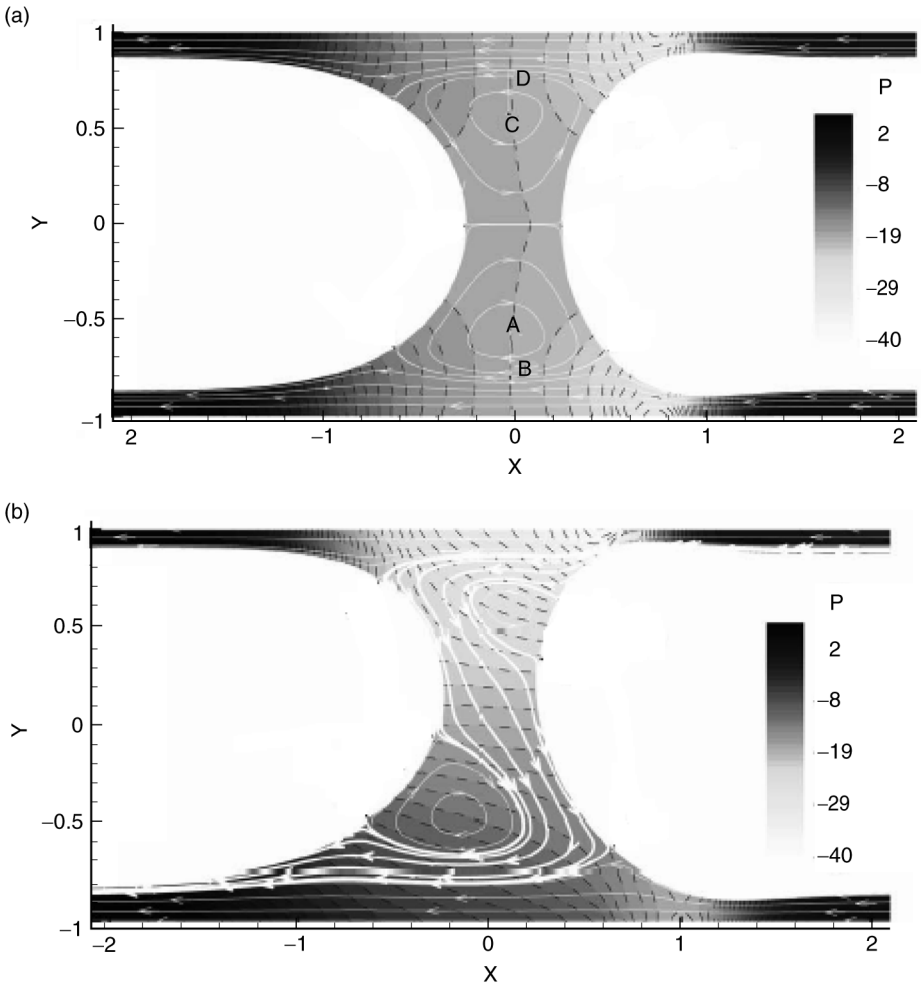

Figure 6. Effect of gravity in horizontal microchannels (taken from (Zheng *et al.*, 2007)) (a) *Bo* = 0 (b) *Bo* = 0.6. The greyscale contour plot shows pressure and the dashed lines are constant pressure lines. The white solid lines with arrows are streamlines.

ΔP_{Slug} is the frictional loss due to the liquid slug and can be assumed to be the sum of the fully-developed laminar flow pressure drop in the liquid and an additional pressure drop caused by the internal recirculation. ΔP_{Film} is the frictional loss in the liquid film and is often neglected in comparison with the pressure drop in the liquid slug (Kreutzer *et al.*, 2005b). In his analytical solution using lubrication approximation, Bretherton (1961) showed that ΔP_{Cap}, the pressure drop over the front and rear bubble caps, for small Capillary numbers in circular capillaries is given by eqn (6) below.

$$\Delta P_{cap} = 7.16\ (3\ Ca)^{2/3}\ \frac{\sigma}{d} \tag{6}$$

Kreutzer et al. (2005b) investigated the pressure drop in Taylor flow experimentally and numerically, and found that the total pressure drop can be calculated by summing up fully-developed liquid-only pressure drop and pressure drop from Bretherton's correlation given by eqn (6) in the case of negligible inertia. They suggested the expression given by eqn (7) for the pressure drop in Taylor flow when inertial effects are significant ($100 < Re < 1000$).

$$\frac{\Delta P}{L} = \varepsilon_L \frac{4}{d}\left(\frac{1}{2}\rho_L U_{TP}^2\right)\frac{16}{Re}\left(1 + a\frac{d}{L_S}\left(\frac{Re}{Ca}\right)^{2/3}\right) \tag{7}$$

The value of the constant a was found to be 0.07 and 0.17 from CFD calculations and experimental measurements, respectively. Walsh *et al*. (2009) confirmed the form of the additional pressure drop term from their experiments and the value of the constant a was an average of the numerically and experimentally obtained values of Kreutzer *et al*. (2005b). Kreutzer *et al*. (2005b) attributed the difference in the value of a in simulations and experiments to the possible impurities present in the liquid. Walsh *et al*. (2009) attributed the difference in the values of a to the variation of the viscosity with temperature.

Using lubrication theory, Suresh and Grotberg (2005) concluded that when the gravitational force is small compared with viscous and surface tension forces ($Bo < 1$, $Ca << 1$), the pressure drop across the liquid slug scales as $Ca^{2/3}$; but when the gravitational force is comparable with viscous and surface tension forces, it scales as $Ca^{1/6}$.

4.5. Heat Transfer

While there has been a lot of research aimed at understanding the hydrodynamics and mass transfer behaviour in Taylor flow, very few researchers have studied heat transfer without phase change in the gas-liquid slug flow in microchannels.

Prothero and Burton (1961) studied heat transfer in air-water slug flow in capillaries experimentally and found slug flow to be twice as effective in transferring heat as liquid-only flow. Oliver and Wright (1964) and Oliver and Young Hoon (1968) studied heat transfer in gas-liquid slug flow in a channel of diameter 6.4 mm for Newtonian and non-Newtonian liquids. They reported that the heat transfer enhancement for the two-phase slug flow is up to two and half times that obtained for the liquid-only flow. Monde *et al*. (1989; 1995) studied the effect on heat transfer of injecting long air bubbles into subcooled water and ethanol in a vertical rectangular channel of cross-section of 2 mm × 20 mm. They found the heat transfer coefficient to be five times larger than that for the flow without bubbles for the experimental conditions studied. Bao (1995) and Bao *et al*. (2000) investigated convective heat transfer experimentally for air-water flow in a circular channel of 1.95 mm diameter for a constant wall heat flux over a large range of gas and liquid flow rates encompassing slug (Taylor) flow, slug-annular flow and annular flow regimes. They found that the heat transfer was enhanced considerably by the presence of the gas, especially at higher gas and liquid velocities. A sharp jump in the heat transfer rate was observed after a particular gas velocity, which the authors believed corresponded to a flow regime transition to slug-annular flow.

Hetsroni *et al*. (2009) studied flow and heat transfer for air-water flow in triangular-section channels of hydraulic diameter 130 μm and reported that the heat transfer coefficient increases with increasing liquid velocity and decreases with increasing air velocity. However, the values of the Nusselt numbers reported are significantly lower when compared with those for the laminar liquid-only flow, which may relate to an inconsistent definition of the wall and bulk temperatures. Walsh *et al*. (2009) studied heat transfer in laminar slug flow in a channel of 1.5 mm diameter for a constant wall heat flux boundary condition experimentally and found that the Nusselt number increases two-fold when the slug length is decreased from 15d to 2d for the same homogeneous void fraction.

Duda and Vrentas (1971) obtained an analytical solution for unsteady heat transfer to a liquid at low Reynolds number in a cylindrical cavity with recirculating flow induced by relative motion between the fluid and the constant-temperature wall. They showed that the circulation currents can cause substantial heat and mass transfer enhancement if the Péclet number of the system is large enough. This can be thought of as a limiting case of slug flow with flat bubble ends and no liquid film surrounding the bubbles.

Recently, Fukagata *et al*. (2007) and Lakehal *et al*. (2008) have shown computationally that Taylor flow in microchannels can significantly enhance heat transfer compared with that of single phase flow. They used the level-set method to capture the gas-liquid interface. Fukagata *et al*. (2007) studied the flow and heat transfer (without phase change) in a periodic computational domain for a channel of 20 μm diameter using a constant wall heat flux boundary condition. They found the Nusselt number to be up to about twice that for single phase flow for the flow conditions studied. Lakehal *et al*. (2008) investigated the convective heat transfer for gas-liquid flow in a microchannel in the slug flow regime for a constant wall temperature boundary condition and reported that the presence of gas bubbles increases the heat transfer rate by three to four times above that of the liquid-only flow.

He *et al*. (2010) studied numerically the heat transfer in a Taylor flow and proposed a mechanistic heat transfer model. The model is based upon one-dimensional, unsteady conduction heat transfer in the continuous liquid film (surrounding the gas bubble as well the recirculating liquid slug) with a time-dependent heat transfer rate at the interface between the film and the liquid plug or bubble. The heat transfer coefficient is set to zero between the film and bubble. Using this model, they showed that the overall heat transfer rate depends upon the mean thermal resistances in the film and slug regions, as well as the heat transfer coefficient at the interface between the two. The model could reproduce the heat transfer coefficient obtained from CFD calculations within an error of ~25%. However, the wider validity of this model remains to be investigated.

Gupta *et al*. (2010) studied the flow and heat transfer for air-water Taylor flow numerically in a microchannel for constant wall heat flux and constant wall temperature boundary conditions. The average Nusselt number obtained for both the conditions was ~2.5 times higher than that obtained from single-phase fully-developed flow. The Nusselt number increased with decreasing homogeneous void fraction and remained almost constant with an increase in the mixture velocity for the range of mixture velocity studied. They pointed out that the radial flow at the nose and tail of the bubbles and the presence of the developing flow in the liquid slug enhance the heat transfer rate beyond that of single-phase fully-developed flow.

4.6. Taylor Flow in Non-Circular Channels

Taylor flow in non-circular channels, such as triangular, rectangular (Kolb and Cerro, 1991; Fries *et al*., 2008; Yue *et al*., 2009) and elliptical (Hazel and Heil, 2002) has also been studied due to its importance in MEMS, Lab-on-a-chip, electronics and biomedical applications. In non-circular channels the bubble is axi-symmetric only at large Capillary numbers and becomes asymmetric at lower Capillary numbers. For example, Kolb and Cerro (1991) found the bubble shape to be axi-symmetric for Capillary numbers ~0.1 or higher and asymmetric for lower Capillary numbers in a rectangular channel. Using numerical simulations Hazel and Heil (2002) showed that at low Capillary numbers, the bubble is axi-symmetric at the nose and a noticeable asymmetry developed downstream of the bubble nose at all values of the Capillary number studied. The asymmetry decays with increasing distance from the bubble nose. A secondary flow from the channel centre to the corners in a plane normal to the channel axis was also observed and the corner liquid film was significantly thicker than that at the centre. At very low values of Capillary numbers, dry-out may also occur at the centre of the channel wall. Fries *et al*. (2008) found that the corner film thickness in a rectangular channel decreases slightly with Ca while the film thickness at the centre remained constant.

4.7. Taylor Flow in Curved Channels

Taylor flow in curved channels can give rise to an interesting flow having recirculating motion in the streamwise direction (as seen in Taylor flow in straight channels) as well as in the spanwise direction (originating from the centrifugal force) and can therefore have very high rates of heat and mass transfer. There are only a few studies available in the literature that address Taylor flow in curved microchannels. Fries *et al*. (2008) studied the flow field in meandering channels having rectangular cross-sections using micro-PIV measurements. They found that the two counter-rotating vortices symmetrical to the channel centreline, characteristic of Taylor flow in straight channels, changed to two different sized vortices providing strong mixing over the centreline. They showed that the liquid velocity field is dependent on the channel geometry and gas and liquid flow rates. The asymmetric motion can be enhanced by increasing the superficial liquid velocity.

Muradoglu and Stone (2007) studied the motion of large bubbles in curved channels analytically using the lubrication approximation and computationally using a front tracking method. The analytical solution showed that the liquid film was thinner on the inside of the bend than on the outside. The bubble velocity relative to the average liquid velocity in a curved channel was always greater than that in a corresponding straight channel and increased monotonically with increasing channel curvature. Numerical computations performed in a two-dimensional computational domain were in good agreement with the analytical solution for small Capillary numbers and small or moderate channel curvatures. For moderate Capillary numbers ($Ca > 0.01$) the numerically calculated film thicknesses were similar to those obtained in a straight channel.

Dogan *et al*. (2009) studied the mixing of two liquids in a serpentine, two-dimensional computational domain numerically using a front-tracking method. Passive tracer particles were

used to visualize and quantify the mixing and thus only convective mixing was quantified. It was observed that chaotic mixing occurs due to the recirculation within the liquid slug as it moved through the winding channel.

In all of the studies available in the literature, only the motion in the streamwise direction could be studied and no information is available on the secondary flow in a plane normal to the channel centreline. Detailed three-dimensional modelling is required to study the details of the Taylor flow in curved microchannels.

5. TOOLS AND TECHNIQUES

Several approaches, such as experimental, theoretical and numerical or a combination of these, have been used to study gas-liquid two-phase flow in microchannels. In this section these techniques are reviewed briefly.

5.1. Experimental Techniques

The small physical dimensions of micro-structured devices necessitate the use of non-intrusive techniques to measure the flow characteristics and the dynamic nature of the multiphase flow imposes the requirement of temporal resolution of flow characterization techniques. Several imaging techniques are used to study such flows in microchannels. Brightfield microscopy, in which the object is illuminated by white light from below and observed from above, with sufficiently short camera shutter time (~10 ms) is the most often used technique. If at least one of the liquid phases is labeled with a fluorescent dye, fluorescent microscopy captures the phase distribution and the shape of the fluid interface.

Particle image velocimetry (PIV), in which one of the liquid phases is seeded with similar density particles and distribution of these particles is recorded at two instants of time and from the change of the particle distribution over time, the flow motion is determined. Santiago *et al*. (1998) introduced micro-PIV, a modified PIV technique for microscale measurements, where the entire flow field is illuminated by a volume of light, unlike the sheet illumination in conventional PIV. The details of the various micro-PIV techniques, its applications and guidelines can be found in a recent review (Lindken *et al*., 2009). Several research groups (Günther *et al*., 2004; King *et al*., 2007; Steijn *et al*., 2007; Fries and von Rohr, 2009) have used micro-PIV technique to study the hydrodynamics of Taylor flow.

5.2. Theoretical Analysis

The fundamental principles of conservation of mass, momentum and energy, in varying degrees of complexity, have been used to understand the transport phenomena in slug flow in microchannels. For example, Suo and Griffith (1964), Thulasidas *et al*. (1995; 1997) and Warnier *et al*. (2008) developed models using a simple one-dimensional continuity equation. By applying overall and species mass conservation various models were developed to study axial dispersion in Taylor flow (Begg, 1971; 1972; Snyder and Adler, 1976a; 1976b; Warnier *et al*., 2008). In his classical paper, Bretherton (1961) studied the hydrodynamics of Taylor flow by solving the two-dimensional (planar and axi-symmetric) Navier-Stokes equations neglecting the non-linear inertial term and using the lubrication approximation. When the inertial term cannot be neglected, the Navier-Stokes equations become non-linear and cannot be solved analytically.

5.3. Numerical Techniques

The non-linear Navier-Stokes equations can be solved analytically in only a few special cases and therefore numerical techniques are required to solve these equations for more general cases. With the exponential increase in computational power during the last few decades, these non-linear equations can be solved and with this branch of fluid mechanics being known as Computational Fluid Dynamics (CFD). CFD analysis is used to understand the hydrodynamics and heat transfer in multiphase flows in microchannels. Slug flow has a large gas-liquid interface and therefore interface-capturing methods, such as Volume of Fluid (VOF) or level-set, have been used to model Taylor flow in microchannels. The equations and methods used are described in detail in the next section.

6. NUMERICAL SOLUTION METHODS APPLIED TO TAYLOR FLOW

While experimental measurements can provide global data, such as pressure drop and overall heat

and mass transfer coefficients; mathematical modelling can give detailed flow, temperature and concentration fields. In theory, the modelling of transport processes becomes more reliable in microchannels as the flow is generally laminar and no heuristic model is required for turbulence modelling. In section 6.1, the governing equations and boundary conditions for two-phase flow and heat transfer (without phase change) are presented. Section 6.2 describes several techniques that are able to capture the location of the gas-liquid interface. Finally, various approaches to the modelling of Taylor flow in microchannels are discussed in section 6.3.

6.1. Governing Equations and Boundary Conditions

Two-phase flow and heat transfer can be represented by the mass, momentum and energy conservation equations for each phase given by eqns (8)–(10). The main assumptions made in the derivation of these equations are:

1. The flow is incompressible.
2. All the fluids are Newtonian.
3. There is no phase change. This is valid when the vapour pressure of the liquid is small compared with the atmospheric pressure and the evaporation of liquid, or equivalently when the fluid temperature is much lower than the local saturation temperature.
4. The fluids are immiscible. For example, the solubility of the gas in the liquid is negligible.
5. Viscous dissipation is neglected.

Continuity:

$$\frac{\partial(\alpha_i \rho_i)}{\partial t} + \nabla .\ (\alpha_i \rho_i \boldsymbol{v}_i) = 0 \tag{8}$$

Momentum:

$$\frac{\partial(\alpha_i \rho_i \boldsymbol{v}_i)}{\partial t} + \nabla .\ (\alpha_i \rho_i \boldsymbol{v}_i \otimes \boldsymbol{v}_i) = -\alpha_i \nabla P_i + \nabla .\ (\alpha_i \boldsymbol{\tau}_i) + \alpha_i \rho_i \boldsymbol{g} + \boldsymbol{F}_{ij} \tag{9a}$$

where

$$\boldsymbol{\tau}_i = \mu_i (\nabla \boldsymbol{v}_i + \nabla \boldsymbol{v}_i^T) \tag{9b}$$

Energy:

$$\frac{\partial(\alpha_i \rho_i e_i)}{\partial t} + \nabla .\ (\alpha_i \rho_i \boldsymbol{v}_i h_i) = \nabla .\ (\alpha_i k_i \nabla T_i) \tag{10}$$

where $i = 1, 2$ denotes the phases. α_i is the volume fraction, ρ_i is the density, μ_i is the dynamic viscosity and k_i is the thermal conductivity of the i^{th} phase. $\boldsymbol{v}_i$, P_i, T_i, e_i and h_i are the velocity, pressure, temperature, internal energy and enthalpy of the i^{th} phase. $\boldsymbol{g}$ is the acceleration due to gravity, t is time and the $\boldsymbol{F}_{ij}$ denotes the momentum transfer between the phases.

6.2. Boundary Conditions

6.2.1. Walls

For viscous flows, the no-slip condition, i.e. the tangential velocity of the fluid is same as that of the wall, is generally imposed at the wall.

$$\boldsymbol{n} \times (\boldsymbol{v} - \boldsymbol{v}_w) = 0 \tag{11}$$

For an impermeable wall, there is no flow normal to the wall surface.

$$\boldsymbol{n} \cdot \boldsymbol{v} = \boldsymbol{n} \cdot \boldsymbol{v}_w \tag{12}$$

6.2.2. Interface Conditions

For two fluids separated by an interface, the velocity field of each fluid must satisfy the continuity of tangential velocity at the interface.

$$\boldsymbol{n} \times (\boldsymbol{v}_1 - \boldsymbol{v}_2) = 0 \tag{13}$$

where $\boldsymbol{v}_1$ and $\boldsymbol{v}_2$ are the velocities at the interface in the two fluids.

At an interface between two fluids an additional condition is required to determine the motion of the surface itself. This condition arises from a momentum balance across the interface which requires that the jump in surface traction combined with momentum fluxes is balanced by the surface tension force. The normal and tangential components of this condition are given by equations (14) and (15), respectively. In the direction normal to the interface, the difference in the normal stresses must be balanced by the surface tension force. In the tangential direction, the tangential components of the shear stresses are balanced by the Marangoni stresses (the stress generated due to a variation in the surface tension coefficient with position). In most simulations, the surface tension coefficient is assumed to be a constant and therefore the gradient term on the right hand side of equation (14) is zero.

$$-P_2 + P_1 + \boldsymbol{n}.\,(\boldsymbol{\tau}_2 - \boldsymbol{\tau}_1) = \sigma\kappa \tag{14}$$

$$\boldsymbol{n} \times (\boldsymbol{\tau}_2 - \boldsymbol{\tau}_1) = \nabla\sigma \tag{15}$$

where σ is the surface tension coefficient and κ is the curvature of the interface.

6.3. Multiphase Flow Modelling Techniques

Several approaches, such as the Eulerian-Eulerian approach, the Eulerian-Lagrangian and the single-fluid formulation can be used to model multiphase flows. The suitability of a particular method for the modelling of a multiphase flow problem depends on the flow characteristics, length-scales, etc. involved. This article is concerned with Taylor flow modelling; therefore only those methods in which the interface can be explicitly captured are described.

6.3.1. Boundary Integral Method

Boundary integral methods are useful for solving those multiphase flow problems in which Stokes-flow (low *Re*; for example flow around droplets or rigid particles) or potential-flow (high *Re*; for example flow field around an airplane wing) approximations are applicable. For both of these cases, the velocity field can be represented by linear governing equations. These linear equations of motion are re-formulated into a system of integral-differential equations and the given boundary conditions are used to set boundary values. The integral equation can then be used to calculate the solution at any desired point in the domain. Martinez and Udell (1989; 1990) and Tsai and Miksis (1994) have used boundary integral methods to model slug flow.

6.3.2. Finite Element Methods

The Galerkin finite-element method can also be used to study the flow field around the bubble in the Taylor flow regime. The role of the gas is assumed to be negligible and the problem is solved as a free-surface problem. In this method the flow equations are solved in the liquid and the gas-liquid boundary is moved in such a manner so that the interface conditions are satisfied. The computational grid consists of two kinds of elements. The grid nodes near the interface which are allowed to move along spline curves and the mesh away from the interface which is kept fixed. Several researchers (Edvinsson and Irandoust, 1996; Giavedoni and Saita, 1997; 1999; Kreutzer *et al*., 2005b; Feng, 2009) have used this type of finite element method to simulate Taylor flow.

6.3.3. Interface Capturing Methods

Interface capturing methods are suitable for multiphase flows in which the interface can be explicitly captured, for example when the interface is larger than the grid size. In interface capturing (and tracking) methods, a single fluid formalism is employed, i.e. only a single set of conservation equations are solved and the interface is tracked using an additional advection equation. The homogeneous flow assumption can be made, i.e. all the fluids are assumed to have the same velocity, pressure and temperature fields. The governing equations for the two phases can be added to give a single-set of equations, as given by eqns (16)–(18). The bulk properties of the

fluid in these equations are the volume fraction weighted average of the properties of the two fluids. An additional equation for a colour function (C) (eqn (19)) is solved to identify the interface location and to calculate the volume fractions.

$$\frac{\partial \rho}{\partial t} + \nabla \cdot (\rho \boldsymbol{v}) = 0 \tag{16}$$

$$\frac{\partial (\rho \boldsymbol{v})}{\partial t} + \nabla \cdot (\rho \boldsymbol{v} \otimes \boldsymbol{v}) = -\nabla P + \nabla \cdot (\mu (\nabla \boldsymbol{v} + \nabla \boldsymbol{v}^T)) + \boldsymbol{F}_{SV} + \boldsymbol{g} \tag{17}$$

$$\frac{\partial (\rho e)}{\partial t} + \nabla . (\rho \boldsymbol{v} h) = \nabla . (k \nabla T) \tag{18}$$

$$\frac{\partial C}{\partial t} + \boldsymbol{v} \cdot \nabla C = 0 \tag{19}$$

This colour function is defined in different ways in different interface capturing techniques. The Volume of fluid (VOF), level-set method, phase-field method and markers point method are some of the most popular techniques. In addition to these, the Lattice Boltzmann method has also been used to model multiphase flow in microchannels. This section discusses briefly such techniques, and their applications in the modelling of Taylor flow in microchannels. Recently, Fletcher *et al.* (2009) have reviewed the CFD modelling of microchannel flows and pointed out that the main challenges in the modelling of multiphase flow in microchannels are the correct identification of the interface location and the minimisation of the parasitic currents near the interface that arise due to surface tension modelling.

The Continuum Surface Force (CSF) model proposed by Brackbill *et al.* (1992) is widely used to model the surface tension effects at the phase interface. The CSF model approximates the surface tension induced stress change by a body force which acts throughout a small but finite fluid region surrounding the interface. The surface tension force per unit area is represented as

$$\boldsymbol{F}_{SV} = \sigma \kappa \delta (\boldsymbol{r} - \boldsymbol{r}_{\text{int}}) \boldsymbol{n} \tag{20}$$

where σ is surface tension coefficient, κ is the radius of curvature, $\delta(\boldsymbol{r}-\boldsymbol{r}_{int})$ is the Dirac delta function and $\boldsymbol{n}$ denotes the unit normal vector at the interface. The normal, $\boldsymbol{n}$, and the curvature, κ in equation (20) are defined in terms of the colour function, C, via;

$$n = \frac{\nabla C}{|\nabla C|}; \kappa = \nabla \cdot n \tag{21}$$

This implementation of the surface tension force can induce unphysical velocities near the interface, known as 'spurious or parasitic currents' (Lafaurie *et al*., 1994; Harvie *et al*., 2006). This occurs because the pressure and viscous force terms do not exactly balance the surface tension force. The accurate calculation of gradients can help in minimising these spurious currents. Tryggvason *et al*. (2007) suggested that in order to avoid the parasitic currents, the normal vector $\boldsymbol{n}$ should be discretised in the same way as the pressure gradient. Recently, Harvie *et al*. (2006) have shown that under certain circumstances these parasitic currents do not decrease in magnitude with mesh refinement or decreased computational time step and can have a significant magnitude in certain circumstances. Therefore, in flows involving surface tension great care must be taken to assess the importance of these effects.

6.3.3.1. Volume-of-Fluid (VOF) Method

The Volume of Fluid (VOF) method (Hirt and Nichols, 1981) is a popular technique to track the gas-liquid interface. In the VOF method, the two fluids are represented via a volume fraction and the location of the interface is tracked by solving the advection equation for the volume fraction of

one of the fluids, α ($0 < \alpha < 1$). Thus, the colour function in eqn (19) is the volume fraction of one of the fluids (α). The gas-liquid interface can be captured either by using geometrical reconstruction schemes (Youngs, 1982; Rudman, 1997; Rider and Kothe, 1998) or by using methods that use high order difference schemes to prevent smearing of interfaces (Ubbink and Issa, 1999). In geometrical reconstruction schemes, such as the commonly used piecewise linear reconstruction scheme (PLIC) (Youngs, 1982), the interface is approximated by a straight line segment in each cell. The orientation of the line is determined by the normal to the interface, which is found by considering the average value of α in the cell under consideration, as well as the neighbouring cells. The surface tension force is then calculated using the CSF model. The commercial CFD software package, ANSYS Fluent uses geometric reconstruction techniques, such as PLIC, to define the interface, while ANSYS CFX uses a compressive differencing scheme to keep the interface sharp.

The VOF method has been used successfully to solve complex problems. However, in the VOF method with a compressive differencing scheme, the interface is diffused over 3–4 cells. In VOF methods using geometric reconstruction techniques the interface is diffused only over 1 cell, so that the interface shape and consequently the applied surface tension force depend strongly on the grid size and aspect ratio.

Ozkan *et al*. (2007) compared the performances of the commercial CFD packages ANSYS CFX, ANSYS Fluent, STAR-CD and their in-house code TURBIT-VOF in modelling a co-current bubble-train flow in a square vertical mini-channel. The computations were based on the VOF method using either a geometrical reconstruction scheme (ANSYS Fluent, TURBIT-VOF) or high-order difference schemes (ANSYS CFX, STAR-CD). The VOF methods using the PLIC scheme gave similar and consistent results, while the use of high order difference schemes showed some deficiencies. The methods based on geometric interface reconstruction were able to resolve and maintain the thin liquid slug, but the rate of smearing associated with the compressive difference scheme VOF methods resulted in artificial bubble coalescence or breakdown of the simulation.

6.3.3.2. Level-Set Method

Another widely used interface capturing method is the level-set method, introduced by Osher and Sethian (1988) and further improved by Sussman *et al*. (1994). In the level-set method, the interface is represented by a level-set function (ϕ), which takes the role of the colour function (C) in eqn (19). This level-set function (ϕ) assumes positive values in one fluid and negative values in the other and the interface is represented as the surface on which the value of the level-set (ϕ) is zero. The absolute value of the level-set function (ϕ) measures the shortest distance from the given location to the interface. The volume fraction (α) is calculated from a smoothed Heaviside function. The surface tension force is calculated using the CSF method. The computation of the normal and curvature in the level-set method can be as accurate as required (e.g. second order accurate or higher).

One of the advantages of the level-set method is its simplicity, especially when computing the curvature (κ) of the interface. After an advection step, the zero of the level-set function represents the interface correctly but the level-set function ceases to be a distance function. The magnitude of the gradients of the level-set function can become very large or very small near the zero value of the level-set function. These large level-set function gradients may cause loss of accuracy of the level-set function advection equation and of variables dependent on it. Re-initialisation of the level-set function helps in maintaining the level-set as a signed distance function (Sussman *et al*., 1994). The primary disadvantage of this method is that the level-set function advection equation is prone to more numerical errors than in VOF methods when the interface undergoes severe stretching or tearing (Rider and Kothe, 1998). This results in the loss of mass conservation and therefore mass conservation needs to be enforced when using this method. Recently, Nourgaliev *et al*. (2005) have suggested that the mass conservation in level-set methods can be significantly improved by reducing the spatial discretization errors by using a high order discretization scheme to solve the advection equation and by increasing the mesh resolution near an interface. TransAT (www.ascomp.ch) and COMSOL (www.comsol.com), a multiphysics code, have incorporated the level-set method to model multiphase flow.

6.2.3.3. Phase Field Method

The phase field method was originally developed to study phase transition phenomena, such as

nucleation, evaporation and solidification (Cahn and Hilliard, 1958; Cahn, 1965), where the diffused interface provides a mean description of the density profile. Recently, the method has been successfully used for the modelling of multiphase flows (Anderson *et al*., 1998; Jacqmin, 1999; 2000; Jamet *et al*., 2001). The phase-function (C') is used to identify different fluids and is updated using a non-linear advection-diffusion equation, known as the Cahn-Hilliard equation. The phase-field convection-diffusion equation is written as

$$\frac{\partial C'}{\partial t} + \boldsymbol{v} \cdot \boldsymbol{\nabla} C' = \boldsymbol{\nabla} \cdot (\Lambda(C') \boldsymbol{\nabla} \varphi) = \boldsymbol{\nabla} \cdot (\Lambda(C') . \boldsymbol{\nabla} (\beta' \psi'(C') - \alpha' \boldsymbol{\nabla}^2 C')) \tag{22}$$

where Λ is the diffusion parameter, called the mobility, φ is the chemical potential which is the rate of change of free energy with respect to C'. $\psi(C')$ models the immiscibility of the two phases and has two minima corresponding to two stable states. Eqn (22) has an additional diffusion term when compared with the colour function advection equation (eqn (19)) used in the VOF and level-set methods. The surface tension force ($\boldsymbol{F}_{SV}$) at the interface is represented by ($-C' \boldsymbol{\nabla} \varphi$). This term is based upon a properly selected free-energy function $\psi(C')$ ensuring that the thickness of the interface remains of the same order as the grid spacing. The frequently used and simplest choice for $\psi(C')$ is $(C' + 1/2)^2/(C' - 1/2)^2$ (Jacqmin, 1999). Unlike the VOF and level-set methods, the phase-field method is based upon models of the fluid's free energy and the interface is described in a thermodynamically consistent manner. COMSOL allows the user to model multiphase flows using this method.

6.3.3.4. Marker Points Method

In the marker points method (Unverdi and Tryggvason, 1992), the interface is tracked by the advection of marker (control) points. These points mark the centre of the smeared interface and the complete interface is defined by connecting the marker points by curves or lines (two-dimensional case) and triangular surface (in three dimensional cases). Changes in the fluid properties across the interface are smoothed out so as to take place over a few grid cells. The surface tension force is calculated at the marker point positions and is distributed to the fixed grid. To compute the surface tension force in a two-dimensional flow, the following approach is used:

$$\boldsymbol{F}_{SV} = \int_{\Delta s} \sigma \kappa \boldsymbol{n} \, ds = \sigma \int_{\Delta s} \frac{\partial \boldsymbol{t}}{\partial s} ds = \sigma (\boldsymbol{t}_2 - \boldsymbol{t}_1) \tag{23}$$

Thus only the calculation of the tangent at the points on the interface is required. This can be achieved by fitting a polynomial to the interface points and differentiating it to obtain the tangent vectors. The main disadvantage of this method is that when the interface is stretched or compressed by the flow, managing the addition or deletion of marker points becomes a difficult task (Unverdi and Tryggvason, 1992).

6.3.4. Lattice Boltzmann Methods

Apart from the conventional continuum CFD methods, lattice Boltzmann methods (LBM) based on the molecular description of fluids have also been used to model gas-liquid two phase flow in microchannels. The LBM is very easily implemented in parallel computing as all of the information exchange is local in time and space. LBM models the flow of a fluid consisting of fictitious particles, with these particles undergoing consecutive propagation and collision processes on a discrete lattice mesh. The following lattice Boltzmann equation is solved for a fluid with a total of n components.

$$f_i^{\sigma}(x + c_i \Delta t, t + \Delta t) - f_i^{\sigma}(x,t) = \Omega_i^{\sigma}(x,t); \; i = 0.1 \ldots m; \sigma = 1, 2, \ldots n \tag{24}$$

where $f_i^{\sigma}(x,t)$ is the particle distribution function representing the number of particles found in the phase space volume element for the σ^{th} component and c_i ($i = 0,1,2 \ldots m$) are the possible velocities a particle can have in order to move from a lattice site to one of its m nearest neighboring sites at

each time step. Ω_i is the collision term and involves the two-particle distribution function f_{12} which further requires f_{123} and so on. For the closure of this equation, the collision operator needs to be modelled. The simplest model for the complicated integral collision operator is often given by the so-called BGK (Bhatnagar-Gross-Krook) collision operator (Bhatnagar *et al*., 1954) and is valid for the case of small deviations of the system from the equilibrium state.

$$\Omega_i = -\frac{f_i - f_i^{eqb}}{\tau} \tag{25}$$

where τ is a typical time-scale associated with the collisional relaxation to the local equilibrium and f_i^{eqb} is the equilibrium distribution function. The macroscopic quantities, such as density ρ, and momentum density $\rho\boldsymbol{u}$, are defined as the particle velocity moments of the distribution function, f_i, given by eqns (26).

$$\rho = \sum_i f_i \tag{26a}$$

$$\rho\boldsymbol{u} = \sum_i f_i \boldsymbol{u}_i \tag{26b}$$

These quantities are conserved locally in any collision process. The equilibrium function is chosen so as to reproduce the correct dynamical equations for ρ and $\boldsymbol{u}$.

Several methods, for example, chromodynamic models (Gunstensen and Rothman, 1991), inter-particle potential models (Shan and Chen, 1993), free-energy models (Swift *et al*., 1995) and finite density models (Luo, 1998) have been developed to model multiphase flow with the lattice Boltzmann approach. The inter-particle potential method (Yang *et al*., 2002; Yu *et al*., 2007) and free-energy methods (Graaf *et al*., 2006) have been used to model multiphase flow in microchannels.

6.3.5. Discussion

The finite element or boundary integral methods give a sharp interface but the details of the gas flow field remain unknown and the boundary integral method can only be applied in the Stokes flow regime. Lattice Boltzmann methods are still in development and for multiphase flows which can have large density and viscosity ratios, as occur in gas-liquid flow, are yet to be implemented. The phase field method is relatively new, with work still required to assess its accuracy and its application to multiphase flow modelling is still to be tested. The VOF and level-set methods are the two most frequently used methods, have been tested for various complex multiphase flow problems and are available in commercial CFD software packages.

6.4. Approaches to Modelling Taylor Flow

Fully-developed Taylor flow is an unsteady, periodic flow in the laboratory frame of reference, but is steady in a frame of reference moving with the bubble. As shown in Figure 7, in the latter case the liquid flows past stationary bubbles and the channel wall moves with the bubble velocity. Modelling of fully-developed Taylor flow in a single unit cell in a frame of reference moving with the bubble reduces the computational complexity significantly, as the flow is steady and the computational domain is only one unit cell long. In most of the numerical studies of Taylor flow available in the literature, the flow has been modelled in a reference frame moving with the bubble. With the increase in computational power in the last decade, it has also been possible to model Taylor flow in a laboratory frame of reference and the phenomena associated with developing Taylor flow and the effect of the inlet conditions on bubble break-off can be studied.

6.4.1. Bubble Frame of Reference

In the bubble frame of reference the gas bubble is stationary and the wall moves. The flow is modelled in a unit cell and the length of a unit cell is required to decide the length of the computational domain. An advantage of the modelling of Taylor flow in the bubble frame of reference is that only the liquid phase is present at the inlet and outlet boundaries and the problem arising from the presence of an interface at the inlet and/or exit boundary is removed. However, this approach requires flow parameters, such as the slug length, void fraction and bubble velocity, as input parameters.

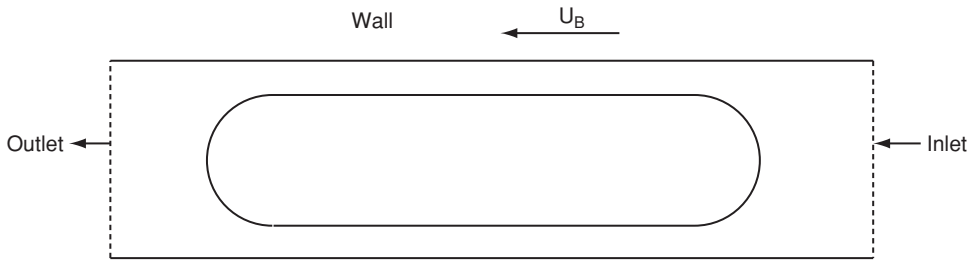

Figure 7. Schematic of Taylor flow in a unit cell in a reference frame moving with the bubble.

The relationship between void fraction (ε_G), bubble velocity (U_B), mixture velocity (U_{TP}) and homogenous void fraction (β) in slug flow in microchannels can be derived by a simple volume balance and is given by eqn (27).

$$\frac{\varepsilon_G}{\beta} = \frac{U_{TP}}{U_B} \tag{27}$$

Some researchers have modelled the flow only in the liquid phase by assuming the gas phase pressure to be uniform; others have included the gas phase in their modelling. In CFD simulations of slug flow in a unit cell, only two of these parameters can be input and the remaining two are calculated as part of the solution. The void fraction (ε_G) is required to be specified initially as the gas volume does not change during the solution. Out of the bubble velocity (U_B) and mixture velocity (U_{TP}), one is specified as an input parameter and the other is calculated as a part of the solution. It is important to note here that the average velocity at any cross-section in the liquid slug is equal to the mixture velocity and not the superficial velocity of the liquid (Suo and Griffith, 1964). If the periodic boundary condition is used at the inlet and outlet, pressure drop over a unit cell can be specified in place of mixture velocity (Fukagata *et al*., 2007).

In gas-liquid Taylor flow, the pressure gradients in the gas phase are negligible when compared with those in the liquid phase. Several researchers (Ratulowski and Chang, 1990; Edvinsson and Irandoust, 1996; Giavedoni and Saita, 1997; 1999; Heil, 2001; de Ryck, 2002; Hazel and Heil, 2002; van Baten and Krishna, 2004; 2005; Kreutzer *et al*., 2005b; Fukagata *et al*., 2007; Feng, 2009) have assumed the gas to be inviscid and the gas pressure to be uniform, allowing them to model the flow in the liquid phase only by applying a no-shear boundary condition at the interface. Modelling solely of the liquid phase is useful only in gas-liquid Taylor flow and cannot be applied in liquid-liquid slug flow, as the bubble liquid cannot be assumed to be inviscid and the assumption of uniform pressure inside the liquid bubble would not be valid.

Some researchers (Halpern and Gaver, 1994; Giavedoni and Saita, 1997; Heil, 2001) have modelled the flow around only the front half of the gas bubble, assuming the bubble to be semi-infinite in length, for a known bubble velocity (as shown in Figure (8)). In such studies, a plug velocity profile is specified at the liquid film end of the bubble and a parabolic velocity profile in

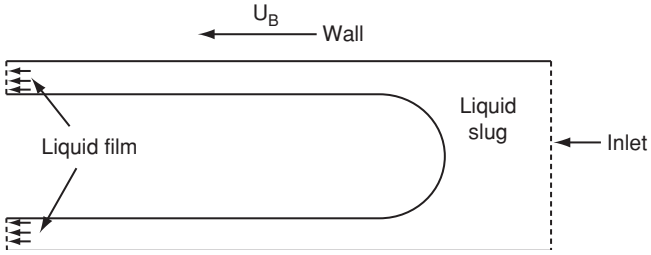

Figure 8. A schematic of the flow around a semi-infinite bubble in a reference frame moving with the bubble.

the liquid slug. The mean velocities at the inlet and outlet are determined analytically in terms of the unknown liquid film thickness and overall mass conservation. The liquid film thickness and the mixture velocity are calculated as a part of the solution. Giavedoni and Saita (1999) also simulated the flow in the rear half of the bubble. Plug flow was assumed in the liquid film side and a parabolic velocity profile which was a function of film thickness was applied at the liquid slug side. The film thickness obtained from the calculations in the front half of the bubble was used (Giavedoni and Saita, 1997).

Some researchers (Edvinsson and Irandoust, 1996; Fujioka and Grotberg, 2004; Kreutzer *et al*., 2005b; Feng, 2009) assumed a bubble shape initially, then used a finite element method to model the liquid flow and calculated the final shape of the bubble by allowing the grid elements near the interface to move. They applied either periodic boundary conditions (with specified mass flow rate or pressure drop) (Edvinsson and Irandoust, 1996) or fully-developed parabolic velocity profile (Kreutzer *et al*., 2005b) at the inlet and exit boundaries. The use of a parabolic velocity profile is justified only when the liquid slug is long enough for fully-developed flow to be obtained.

Multiphase flow methods, which consider both the gas and liquid phases, such as VOF (Taha and Cui, 2004; Akbar and Ghiaasiaan, 2006; 2006; Wang and Liu, 2008), level-set (Fukagata *et al*., 2007), phase field (He *et al*., 2007; He and Kasagi, 2008) and marker point (Muradoglu *et al*., 2007) have all been used to model Taylor flow in a single unit cell in a reference frame moving with the bubble. In some of these studies (Taha and Cui, 2004; 2006; Liu and Wang, 2008) the mixture velocity was specified at the inlet and outflow boundary condition (zero gradient) at the outlet. The wall velocity was guessed initially and then updated iteratively until the bubble no longer moved in the axial direction. Fukagata *et al*. (2007) and He *et al*. (2007) used pressure drop at the periodic boundaries and the bubble velocity was calculated as a part of the simulation.

Taylor flow modelling in a single unit cell in a bubble frame of reference is useful to model fully-developed Taylor flow but some flow parameters, such as void fraction which are not known in advance, need to be assumed.

6.4.2. Laboratory Frame of Reference

Recently several researchers have modelled the flow in the laboratory frame of reference (Yang *et al*., 2002; Qian and Lawal, 2006; Yu *et al*., 2007; Lakehal *et al*., 2008; Narayanan and Lakehal, 2008; Shao *et al*., 2008; Chen *et al*., 2009; Guo and Chen, 2009; Gupta *et al*., 2009; 2010). Modelling of Taylor flow in a laboratory frame of reference requires only the superficial velocities (or mixture velocity and homogeneous void fraction) of the two phases as an input and the void fraction and bubble velocity are calculated as part of the solution. Recently, there has been a lot of interest in controlling the bubble or droplet size, which requires studying the effect of the inlet conditions on bubble break-off. Modelling of flow in a laboratory frame of reference does not require the void fraction and the bubble velocity as input parameters and developing, as well as developed, Taylor flow can be studied.

However, when using such an approach, a long computational domain is required to obtain a fully-developed Taylor flow (Lakehal *et al*., 2008; Gupta *et al*., 2010) requiring in turn a large computational grid in order to capture flow features accurately. As discussed in Gupta *et al*. (2009) several studies (Qian and Lawal, 2006; He *et al*., 2007; Kumar *et al*., 2007; Kashid *et al*., 2008; Goel and Buwa, 2009) have appeared in the literature that use computational grids having insufficient near-wall grid refinement to capture the liquid film, especially at lower Capillary numbers.

The importance of the effect of thin films on the hydrodynamics has been recognised recently. Gupta *et al*. (2009) have made a detailed study of the effect of mesh size and morphology and numerical schemes on the calculated bubble shapes. They showed that poor mesh resolution was responsible for many Taylor flow simulations that have the bubble in direct contact with the wall. Advice on the required grid resolution and aspect ratio needed to correctly capture the liquid film are given. Additional advice for users of ANSYS Fluent was provided on the best choice of schemes and differencing techniques.

TransAT (www.ascomp.ch), a high-accuracy CFD code has incorporated a film boundary condition to capture thin liquid films. After the advection step of the level-set function, the value of the level-set function is extrapolated onto the wall using second-order extrapolation. If the extrapolated value is lower than the specified thickness, the value at the near wall node is set to the specified film thickness and the value next to this node is changed accordingly. Thus, the values at

the wall and the grid elements next to the wall are changed to maintain the film thickness. As only the value at the grid point next to the wall is changed, the specified film thickness should be less than half the near wall grid size.

Thomas *et al*. (2010) introduced a method to account for the thin film effect. The method is based on solving an equation governing the evolution of the film in addition to computing the fully-resolved flow in the computational domain. The additional equation is based on standard assumptions for thin film modelling (constant axial pressure gradient, linear velocity profile) and uses the information (pressure) from the fully-resolved flow. The film modelling results are then used to modify the wall boundary condition. This model is applied only when the film thickness is smaller than the near wall grid size.

7. CONCLUSIONS AND RECOMMENDATIONS

It is clear from the number of studies presented in this paper that Taylor or slug flow is being studied in great detail both experimentally and numerically. This reflects its importance, in terms of the large range of conditions for which it occurs and for the desirable properties of this flow regime for lab-on-a-chip applications or chemical reaction studies where there is no back-mixing. Whilst transport phenomena in Taylor flow are generally well understood there remain some gaps. However, there are promising trends in experimental and modelling work that will further increase our knowledge of this flow regime in the near future.

- Experimental advances are allowing more accurate and detailed measurements of the flow characteristics to be obtained and will therefore provide more and better data for model validation. Areas of progress include determination of the liquid film thickness, the velocity profile in the slugs, heat transfer rates and local temperatures. Such data will be invaluable in further validating CFD results.
- Experiments have shown that in millimetre-size horizontal channels, gravitational forces can give rise to an asymmetric liquid film distribution around the bubble in some circumstances. However, it is not well understood what effect gravity has on the bubble shape, flow field and heat transfer behaviour.
- There have been some studies of Taylor flow in non-circular channels and/or tortuous flow paths but there needs to be further experimental work to provide detailed velocity and heat transfer data for model validation. Three dimensional numerical simulations are required to determine how the flow and heat transfer behaviour are modified by non-circular channels and the presence of bends in tortuous passages.
- There are a growing number of numerical techniques that can be used to study Taylor flow. There has been a progression from single phase simulations in which the gas bubble was not captured, to front tracking methods using the VOF or level set methods to capture the gas-liquid interface. New techniques, such as the phase field and Lattice Boltzmann methods, hold promise for more accurate solutions in the future because they can include surface tension effects more accurately.
- The liquid film at the wall has not been captured successfully in many CFD modelling studies of Taylor flow using interface capturing techniques, largely due to poor resolution of the flow near the wall. This deficiency of the numerical simulation has a profound effect on the calculated frictional pressure drop and the heat and/or mass transfer rates to the wall.
- Recent work has shown that this problem of numerical dry-out can be avoided using properly constructed numerical grids and algorithms. The increasing performance of computers and CFD codes will allow more accurate simulations to be made.
- Most simulations are currently two dimensional because of the large computational resource requirements needed for three dimensional simulations. However, as computational power grows, and solution algorithms are improved, it will be possible to solve for three dimensional flow in non-straight channels with gravitational forces included.
- Experimental studies show that the manner in which the gas and liquid are brought into contact has a significant effect on the bubble and slug lengths. Numerical techniques need to be developed to allow CFD simulations to produce Taylor flow with pre-determined characteristics, such as bubble and slug lengths.

- Many aspects of heat and mass transfer in Taylor flow remain to be explored and will require developments in both experimental methods and numerical simulation techniques before they can be fully quantified.

ACKNOWLEDGEMENTS

The Heatric division of Meggitt (UK) Ltd and the Australian Research Council are thanked for their financial support of this work. R. Gupta also acknowledges the University of Sydney's Henry Bertie and Florence Mabel Gritton Research Scholarship Foundation.

REFERENCES

Afkhami, S., S. Zaleski and M. Bussmann (2009). "A mesh-dependent model for applying dynamic contact angles to VOF simulations." *Journal of Computational Physics* 228: 5370–5389.

Ajaev, V. S. and G. M. Homsy (2006). "Modeling shapes and dynamics of confined bubbles." *Annual Review of Fluid Mechanics* 38: 277–308.

Akbar, M. K. and S. M. Ghiaasiaan (2006). "Simulation of Taylor flow in capillaries based on the volume-of-fluid techniques." *Industrial & Engineering Chemistry Fundamentals* (45): 5396–5403.

Akbar, M. K., D. A. Plummer and S. M. Ghiaasiaan (2003). "On gas-liquid two-phase flow regimes in microchannels." *International Journal of Multiphase Flow* 29: 855–865.

Anderson, D. M., G. B. McFadden and A. A. Wheeler (1998). "Diffuse-interface methods in fluid mechanics." *Annual Review of Fluid Mechanics* 30(1): 139–165.

Angeli, P. and A. Gavriilidis (2008). "Hydrodynamics of Taylor flow in small channels: a review." *Proc. IMechE: Part C: Mechanical Engineering Science* 222: 737–751.

Armand, A. A. (1959). "The resistance during the movement of a two-phase system in horizontal pipes." *Atomic Energy Research Establishment (AERE) Libr. Trans*. 828: 16–23.

Armand, A. A. and G. G. Treschev (1946). "The resistance during the movement of a two-phase system in horizontal pipes." *Izv. Vsev. Teplotak Inst*. 1: 16–23.

Aussillous, P. and D. Quéré (2000). "Quick deposition of a fluid on the wall of a tube." *Physics of Fluids* 12(10): 2367–2371.

Baird, J. R., D. F. Fletcher and B. S. Haynes (2003). "Local condensation heat transfer rates in fine passages." *International Journal of Heat and Mass Transfer* 46: 4453–4466.

Bao, Z. Y., M. G. Bosnich and B. S. Haynes (1994). "Estimation of void fraction and pressure drop for two-phase flow in fine passages." *Trans IChemE, Part A, Chemical Engineering Research and Design* 72: 625–632.

Bao, Z. Y., D. F. Fletcher and B. S. Haynes (2000). "An experimental study of gas-liquid flow in a narrow conduit." *International Journal of Heat and Mass Transfer* 43: 2313–2324.

Barajas, A. M. and R. L. Panton (1993). "The effect of contact angle on two-phase flow in capillary tubes." *International Journal of Multiphase Flow* 19: 337–346.

Barnea, D., Y. Luninski and Y. Taitel (1983). "Flow in small diameter pipes." *Canadian Journal of Chemical Engineering* 61: 617–620.

Bayraktar, T. and S. B. Pidugu (2006). "Characterisation of liquid flow in microfluidic systems." *International Journal of Heat and Mass Transfer* 49: 815–824.

Beattie, D. R. H. and P. B. Whalley (1982). "A simple two-phase frictional pressure drop calculation method." *International Journal of Multiphase Flow* 8: 83–87.

Begg, R. D. (1971). "Dynamics of Continuous Segnmented Flow Analysis." *Analytical Chemistry* 43(7): 854–857.

Begg, R. D. (1972). "Concentration Effects in a Dynamic Model of the Technicon Autoanalyzer." *Analytical Chemistry* 44(3): 631–632.

Bertsch, S. S., E. A. Groll and S. V. Garimella (2008). "Review and Comparative Analysis of Studies on Saturated Flow Boiling in Small Channels." *Nanoscale and Microscale Thermophysical Engineering* 12(3): 187–227.

Bhatnagar, P., E. Gross and M. Krook (1954). "A model for collisional processes in gases I: small amplitude processes in charged and neutral one-component system." *Physical Review* 94: 511.

Brackbill, J. U., D. B. Kothe and C. Zemach (1992). "A continuum method for modeling surface tension." *Journal of Computational Physics* 100(2): 335–354.

Bretherton, F. P. (1961). "The motion of long bubbles in tubes." *Journal of Fluid Mechanics* 10: 166–188.

Buie, C. R. and J. G. Santiago (2009). "Two-phase hydrodynamics in a miniature direct methanol fuel cell." *International*

Journal of Heat and Mass Transfer 52: 5158–5166.

Cahn, J. W. (1965). "Phase Separation by Spinodal Decomposition in Isotropic Systems." *The Journal of Chemical Physics* 42(1): 93–99.

Cahn, J. W. and J. Hilliard, E. (1958). "Free Energy of a Nonuniform System. I. Interfacial Free Energy." *The Journal of Chemical Physics* 28(2): 258–267.

Chen, T. and S. V. Garimella (2006). "Measurements and high-speed visualizations of flow boiling of a dielectric fluid in a silicon microchannel heat sink." *International Journal of Multiphase Flow* 32: 957–971.

Chen, W. L., M. C. Twu and C. Pan (2002). "Gas-liquid two-phase flow in microchannels." *International Journal of Multiphase Flow* 28(7): 1235.

Chen, Y., R. Kulenovic and R. Mertz (2009). "Numerical study on the formation of Taylor bubbles in capillary tubes." *International Journal of Thermal Sciences* 48(2): 234–242.

Chen, Y., M. Shi, P. Cheng and G. P. Peterson (2008). "Condensation in Microchannels." *Nanoscale and Microscale Thermophysical Engineering* 12(2): 117–143.

Chisholm, D. (1967). "A theoretical basis for the Lockhart–Martinelli correlation for two-phase flow." *International Journal of Heat and Mass Transfer* 10: 1767–1778.

Chung, P. M. Y. and M. Kawaji (2004). "The effect of channel diameter on adiabatic two-phase flow characteristics in microchannels." *International Journal of Multiphase Flow* 30(7–8): 735.

Coleman, J. W. and S. Garimella (1999). "Characterization of two-phase flow patterns in small diameter round and rectangular tubes." *International Journal of Heat and Mass Transfer* 42(15): 2869.

Craig, V. S. J., C. Neto and D. R. M. William (2001). "Shear-dependent boundary slip in an aqueous Newtonian liquid." *Phys. Rev. Lett*. 87: 54504–54507.

Damianides, C. A. and J. W. Westwater (1988). *Two-phase flow patterns in a compact heat exchanger and in small tubes*. Proc Second UK National Conference on Heat Transfer, Glasgow, Glasgow, Mechanical Engineering Publications, London.

de Ryck, A. (2002). "The effect of weak inertia on the emptying of a tube." *Physics of Fluids* 14(7): 2102–2108.

Dogan, H., S. Nas and M. Muradoglu (2009). "Mixing of miscible liquids in gas-segmented serpentine channels." *International Journal of Multiphase Flow* 35(12): 1149–1158.

Dukler, A. E., M. I. Wicks and R. G. Cleveland (1964). "Pressure drop and hold-up in two-phase flow." *AIChE Journal* 10: 38–51.

Dutkowski, K. (2010). "Air-Water Two-Phase Frictional Pressure Drop in Minichannels." *Heat Transfer Engineering* 31(4): 321–330.

Edvinsson, R. K. and S. Irandoust (1996). "Finite Element Analysis of Taylor Flow." *AIChE Journal* 42(7): 1815–1823.

Fairbrother, F. and A. E. Stubbs (1935). "The bubble-tube method of measurement." *J. Chem. Soc. 1*: 527–529.

Feng, J. Q. (2009). "A long gas bubble moving in a tube with flowing liquid." *International Journal of Multiphase Flow* 35: 738–746.

Fletcher, D. F., B. S. Haynes, J. Aubin and C. Xuereb (2009). Modelling of microfluidic devices. *Handbook of Micro Reactors. Fundamentals, Operations and catalysts*. V. Hessel, J. C. Schouten, A. Renken and J.-I. Yoshida, Wiley-VCH 1: 117–144.

Friedel, L. (1979). *Improved friction pressure drop correlations for horizontal and vertical two-phase pipe flow*. The European Two-phase Flow Group Meeting, Paper E2, Ispara, Italy.

Fries, D. M., F. Trachsel and P. R. Von Rohr (2008). "Segmented gas-liquid flow characterization in rectangular microchannels." *International Journal of Multiphase Flow* 34: 1108–1118.

Fries, D. M. and P. R. von Rohr (2009). "Liquid mixing in gas-liquid two-phase flow by meandering microchannels." *Chemical Engineering Science* 64(6): 1326–1335.

Fries, D. M., S. Waelchli and P. R. Von Rohr (2008). "Gas–liquid two-phase flow in meandering microchannels." *Chemical Engineering Journal* 135S: S37–S45.

Fujioka, H. and J. B. Grotberg (2004). "Steady propagation of a liquid plug in a two-dimensional channel." *Journal of Biomechanical Engineering* 126: 567–577.

Fukagata, K., N. Kasagi, P. Ua-arayaporn and T. Himeno (2007). "Numerical simulation of gas-liquid two-phase flow and convective heat transfer in a micro tube." *International Journal of Heat and Fluid Flow* 28(1): 72–82.

Fukano, T. and A. Kariyasaki (1993). "Characteristics of gas-liquid two-phase flow in a capillary tube." *Nuclear Engineering and Design* 141(1–2): 59.

Gaver, D. P., D. Halpern, O. E. Jensen and J. B. Grotberg (1996). "The steady motion of a semi-infinite bubble through a

flexible-walled channel." *Journal of Fluid Mechanics Digital Archive* 319(-1): 25–65.

Giavedoni, M. D. and F. A. Saita (1997). "The axisymmetric and plane cases of a gas phase steadily displacing a Newtonian liquid—A simultaneous solution of the governing equations." *Physics of Fluids* 9(8): 2420–2428.

Giavedoni, M. D. and F. A. Saita (1999). "The rear meniscus of a long bubble steadily displacing a Newtonian liquid in a capillary tube." *Physics of Fluids* 11(4): 786–794.

Goel, D. and V. V. Buwa (2009). "Numerical simulations of bubble formation and rise in microchannels." *Industrial & Engineering Chemistry Research* 48: 8109–8120.

Graaf, V. S., T. Nisisako, C. G. P. H. Schroen, R. G. M. vanderSman and R. M. Boom (2006). "Lattice Boltzmann Simulations of Droplet Formation in a T-Shaped Microchannel." *Langmuir* 22(9): 4144–4152.

Gunstensen, A. and D. Rothman (1991). "Lattice Boltzmann studies of immiscible two phase flows through porous media." *Phys. Rev. A* 43: 4320.

Günther, A., M. Jhunjhunwala, M. Thalmann, M. A. Schmidt and K. F. Jensen (2005). "Micromixing of miscible liquids in segmented gas-liquid flow." *Langmuir* 21: 1547–1555.

Günther, A., S. A. Khan, M. Thalmann, F. Trachsel and K. F. Jensen (2004). "Transport and reaction in microscale segmented gas-liquid flow." *Lap on a Chip* 4: 278–286.

Guo, F. and B. Chen (2009). "Numerical study on taylor bubble formation in a microchannel t-junction using vof method." *Microgravity Science and Technology* 21(SUPPL. 1): S51–S58.

Gupta, R., D. F. Fletcher and B. S. Haynes (2009). "On the CFD modelling of Taylor Flow in Microchannels." *Chemical Engineering Science* 64(12): 2941–2950.

Gupta, R., D. F. Fletcher and B. S. Haynes (2010). "CFD Modelling of Heat Transfer in the Taylor Flow Regime." *Chemical Engineering Science* 65(6): 2094–2017.

Gupta, R., P. E. Geyer, D. F. Fletcher and B. S. Haynes (2008). "Thermohydraulic performance of a periodic trapezoidal channel with a triangular cross-section." *International Journal of Heat and Mass Transfer* 51: 2925–2929.

Halpern, D. and D. P. Gaver (1994). "Boundary element analysis of the time-dependent motion of a semi-infinite bubble in a channel." *Journal of Computational Physics* 115: 366–375.

Han, Y. and N. Shikazono (2009). "Measurement of the liquid film thickness in micro tube slug flow." *International Journal of Heat and Fluid Flow* 30(5): 842–853.

Hardt, S., W. Ehrfeld, V. Hessel and K. M. Vanden Bussche (2003). "Strategies for size reduction of microreactors by heat transfer enhancement effects." *Chemical Engineering Communications* 190(4): 540–559.

Harvie, D. J. E., M. R. Davidson and M. Rudman (2006). "An analysis of parasitic current generation in Volume of Fluid simulations." *Applied Mathematical Modelling* 30(10): 1056.

Hazel, A. L. and M. Heil (2002). "The steady propagation of a semi-infinte bubble into a tube of elliptical or rectangular cross-section." *Journal of Fluid Mechanics* 470: 91–114.

He, Q., K. Fukagata and N. Kasagi (2007). *Numerical simulation of gas-liquid two-phase flow and heat transfer with dry-out in a micro tube*. In proceedings: 6th International Conference on Multiphase Flow, Leipzig, germany.

He, Q., Y. Hasegawa and N. Kasagi (2010). "Heat transfer modelling of gas-liquid slug flow without phase change." *International Journal of Heat and Fluid Flow* 31: 126–136.

He, Q. and N. Kasagi (2008). "Phase-Field simulation of small capillary-number two-phase flow in a microtube." *Fluid Dynamics Research* 40(7–8): 497.

Heil, M. (2001). "Finite Reynolds number effects in the Bretherton problem." *Physics of Fluids* 13(9): 2517–2521.

Herwig, H. and O. Hausner (2003). "Critical view on 'New results in micro-fluid mechanics: An example'." *International Journal of Heat and Mass Transfer* 46: 935–937.

Hetsroni, G., A. Mosyak, Pogrebnyak E. and L. P. Yarin (2005). "Fluid flow in micro-channels." *International Journal of Heat and Mass Transfer* 48: 1982–1998.

Hirt, C. W. and B. D. Nichols (1981). "Volume of Fluid (VOF) method for the dynamics of free boundaries." *Journal of Computational Physics* 39: 201–225.

Ho, C. M. and Y. C. Tai (1998). "Micro-Electro-Mechanical-Systems (MEMS) and fluid flows." *Annual Review of Fluid Mechanics* 30(1): 579–612.

Horvath, C., B. A. Solomon and J.-M. Engasser (1973). "Measurement of radial transport in slug flow using enzyme tubes." *Industrial & Engineering Chemistry Fundamentals* 12(4): 431–439.

Ide, H., A. Kariyasaki and T. Fukano (2007). "Fundamental data on the gas-liquid two-phase flow in minichannels." *International Journal of Thermal Sciences* 46(6): 519–530.

Inada, F., D. A. Drew and R. T. Lahey (2004). "An analytical study on interfacial wave structure between the liquid film and gas core in a vertical tube." *International Journal of Multiphase Flow* 30(7–8): 827.

Jacqmin, D. (1999). "Calculation of Two-Phase Navier-Stokes Flows Using Phase-Field Modeling." *Journal of Computational Physics* 155(1): 96–127.

Jacqmin, D. (2000). "Contact-line dynamics of a diffuse fluid interface." *Journal of Fluid Mechanics* 402: 57–88.

Jamet, D., O. Lebaigue, N. Coutris and J. M. Delhaye (2001). "Feasibility of using the second gradient theory for the direct numerical simulations of liquid-vapour flows with phase change." *Journal of Computational Physics* 169: 624–651.

Kashid, M. N., D. F. Rivas, D. W. Agar and S. Turek (2008). "On the hydrodynamics of liquid-liquid slug flow capillary microreactors." *Asia-Pacific Journal of Chemical Engineering* 3(2): 151–160.

Kawahara, A., P. M. Y. Chung and M. Kawaji (2002). "Investigation of two-phase flow pattern, void fraction and pressure drop in a microchannel." *International Journal of Multiphase Flow* 28(9): 1411.

Khan, S. A., A. Gunther, M. A. Schmidt and K. F. Jensen (2004). "Microfluidic Synthesis of Colloidal Silica." *Langmuir* 20: 8604–8611.

King, C., E. Walsh and R. Grimes (2007). "PIV measurements of flow within plugs in a microchannel." *Microfluidics and Nanofluidics* 3: 463–472.

Kohl, M. J., S. I. Abdel-Khalik, S. M. Jeter and D. L. Sadowksi (2005). "An experimental investigation of microchannel flow with internal pressure measurements." *International Journal of Heat and Mass Transfer* 48: 1518–1533.

Kolb, W. B. and R. L. Cerro (1991). "Coating the inside of a capillary of square cross-section." *Chemical Engineering Science* 46(9): 2181–2195.

Koo, J. and C. Kleinstreuer (2004). "Viscous dissipation effects in microtubes and microchannels." *International Journal of Heat and Mass Transfer* 47: 3159–3169.

Kreutzer, M. T., F. Kapteijn, J. A. Moulijn and J. J. Heiszwolf (2005a). "Multiphase monolith reactors: Chemical reaction engineering of segmented flow in microchannels." *Chemical Engineering Science* 60(22): 5895–5916.

Kreutzer, M. T., F. Kapteijn, J. A. Moulijn, C. R. Kleijn and J. J. Heiszwolf (2005b). "Inertial and interfacial effects on pressure drop of Taylor flow in capillaries." *AIChE Journal* 51(9): 2428–2440.

Kumar, V., S. Vashisth, Y. Hoarau and K. D. P. Nigam (2007). "Slug flow in curved microreactors: Hydrodynamic study." *Chemical Engineering Science* 62(24): 7494.

Laborie, C., L. Cabassud and Durand-Bourlier (1999). "Characterisation of gas-liquid two phase flow inside capillaries." *Chemical Engineering Science* 54: 5723–5735.

Lafaurie, B., C. Nardone, R. Scardovelli, S. Zaleski and G. Zanetti (1994). "Modelling Merging and Fragmentation in Multiphase Flows with SURFER." *Journal of Computational Physics* 113(1): 134.

Lakehal, D., G. Larrignon and C. Narayanan (2008). "Computational heat transfer and two-phase flow topology in miniature tubes." *Microfluidics and Nanofluidics* 4(4): 261–271.

Lindken, R., M. Rossi, S. Groβe and J. Westerweel (2009). "Micro-Particle Image Velocimetry (MUPIV): Recent developments, applications and guidelines." *Lab on a Chip* 9: 2551–2567.

Link, D. R., S. L. Anna, D. Z. Weitz and H. A. Stone (2004). "Geometrically Mediated Breakup of Drops in Microfluidic Devices." *Physical Review Letters* 92: 0545031–0545034.

Liu, D. and S. Wang (2008). "Hydrodynamics of Taylor flow in noncircular capillaries." *Chemical Engineering and Processing: Process Intensification* 47(12): 2098.

Liu, H., C. O. Vandu and R. Krishna (2005). "Hydrodynamics of Taylor Flow in Vertical Capillaries: Flow Regimes, Bubble Rise Velocity, Liquid Slug Length, and Pressure Drop." *Industrial & Engineering Chemistry Research* 44(14): 4884–4897.

Lockhart, R. W. and R. C. Martinelli (1949). "Proposed correlations of data for isothermal two-phase two-component flow in pipes." *Chemical Engineering Progress* 45: 39–48.

Luo, L. S. (1998). "Unified theory of lattice Boltzmann for non-ideal gases." *Phys. Rev. Lett*. 81: 1618.

Martinez, M. J. and K. S. Udell (1989). "Boundary integral analysis of the creeping flow of long bubbles in capillaries." *Journal of Applied Mechanics* 56(211–217).

Martinez, M. J. and K. S. Udell (1990). "Axisymmetric creeping motion of drops through circular tubes." *Journal of Fluid Mechanics* 210: 565–591.

Mas, N. D., A. Gunther, M. A. Schmidt and K. F. Jensen (2003). "Microfabricated multiphase reactors for the selective direct fluorination of aromatics." *Industrial & Engineering Chemistry Research* 42: 698–710.

McAdams, W. H., W. K. Woods and L. C. J. Heroman (1942). "Vaporization inside horizontal tubes-II-Benzene-oil

mixtures." *Trans. ASME* 64: 193–200.

Mishima, K. and T. Hibiki (1996). "Some characteristics of air-water two-phase flow in small diameter vertical tubes." *International Journal of Multiphase Flow* 22(4): 703.

Mishima, K., T. Hibiki and H. Nishihara (1993). "Some characteristics of gas-liquid flow in narrow rectangular ducts." *International Journal of Multiphase Flow* 19(1): 115.

Morini, G. L., M. Lorenzini, Colin S. and G. S. (2007). "Experimental analysis of pressure drop and laminar to turbulent transition for gas flows in smooth microtubes." *Heat Transfer Engineering* 28(8&9): 670–679.

Mourik, S. V., A. E. P. Veldman and M. E. Dreyer (2005). "Simulation of capillary flow with a dynamic contact angle." *Microgravity Science and Technology* 17(3): 87–93.

Muradoglu, M., A. Gunther and H. A. Stone (2007). "A computational study of axial dispersion in segmented gas-liquid flow." *Physics of Fluids* 19: 072109–1–11.

Muradoglu, M. and H. A. Stone (2007). "Motion of large bubbles in curved channels." *Journal of Fluid Mechanics* 570: 455–466.

Narayanan, C. and D. Lakehal (2008). "Two-phase convective heat transfer in miniature pipes under normal and microgravity conditions." *Journal of Heat Transfer* 130: 074502–1–074502–5.

Nourgaliev, R. R., S. Wiri, N. T. Dinh and T. G. Theofanous (2005). "On improving mass conservation of level set by reducing spatial discretization errors." *International Journal of Multiphase Flow* 31(12): 1329.

Osher, S. and J. A. Sethian (1988). "Fronts propagating with curvature-dependent speed: algorithms based on Hamilton-Jacobi formulations." *Journal of Computational Physics* 79: 12–49.

Özkan, F., M. Wörner, A. Wenka and H. S. Soyhan (2007). "Critical evaluation of CFD codes for interfacial simulation of bubble-train flow in a narrow channel." *International Journal for Numerical Methods in Fluids* 55(6): 537–564.

Park, H. S. and J. Punch (2008). "Friction factor and heat transfer in multiple microchannels with uniform flow distribution." *International Journal of Heat and Mass Transfer* 51(17–18): 4535.

Pedersen, H. and C. Horvath (1981). "Axial dispersion in a segmented gas-liquid flow." *Industrial & Engineering Chemistry Fundamentals* 20: 181–186.

Pehlivan, K., I. Hassan and M. Vaillancourt (2006). "Experimental study on two-phase flow and pressure drop in millimeter-size channels." *Applied Thermal Engineering* 26(14–15): 1506.

Pohorecki, R., P. Sobieszuk, K. Kula, W. Moniuk, M. Zieliński, P. Cygański and P. Gawiński (2008). "Hydrodynamic regimes of gas–liquid flow in a microreactor channel." *Chemical Engineering Journal* 135S: S185–S190.

Premoli, A., D. Francesco and A. Prina (1970). An empirical correlation for evaluating two-phase mixture density under adiabatic conditions. *European two-phase flow group meeting, Milan*. Milan.

Prothero, J. and A. C. Burton (1961). "The Physics of blood flow in capillaries: I. The nature of the motion." *Biophysical Journal* 1: 565–579.

Qian, D. and A. Lawal (2006). "Numerical study on gas and liquid slugs for Taylor flow in a T-junction microchannel." *Chemical Engineering Science* 61(23): 7609.

Ratulowski, J. and H. C. Chang (1990). "Marangoni effects of trace impurities on the motion of long gas bubbles in capillaries." *Journal of Fluid Mechanics Digital Archive* 210(-1): 303–328.

Rider, W. J. and D. B. Kothe (1998). "Reconstructing volume tracking." *Journal of Computational Physics* 141(2): 112.

Rudman, M. (1997). "Volume-tracking methods for interfacial flow calculations." *International Journal for Numerical Methods in Fluids* 24(7): 671–691.

Saisorn, S. and S. Wongwises (2008). "Flow pattern, void fraction and pressure drop of two-phase air-water flow in a horizontal circular micro-channel." *Experimental Thermal and Fluid Science* 32(3): 748–760.

Salman, W., A. Gavriilidis and P. Angeli (2006). "On the formation of Taylor bubbles in small tubes." *Chemical Engineering Science* 61: 6653–6666.

Santiago, J. G., S. T. Wereley, C. D. Meinhart, C. D. Beebe and R. J. Adrian (1998). "A particle image velocimetry system for microfluidics." *Experiments in Fluids* 25: 316–319.

Schwartz, L. W., H. M. Princen and A. D. Kiss (1986). "On the motion of bubbles in capillary tubes." *Journal of Fluid Mechanics* 172: 259–275.

Serizawa, A., Z. Feng and Z. Kawara (2002). "Two-phase flow in microchannels." *Experimental Thermal and Fluid Science* 26(6–7): 703–714.

Shan, X. and H. Chen (1993). "Lattice Boltzmann model for simulating flows with multiple phases and components."

Physical Review E 47(3): 1815.

Shao, N., A. Gavriilidis and P. Angeli (2009). "Flow regimes for adiabatic gas-liquid flow in microchannels." *Chemical Engineering Science* 64(11): 2749–2761.

Shao, N., W. Salman, A. Gavriilidis and P. Angeli (2008). "CFD simulations of the effect of inlet conditions on Taylor flow formation." *International Journal of Heat and Fluid Flow* 29: 1603–1611.

Sharp, K. V. and R. J. Adrian (2004). "Transition from laminar flow to turbulent flow in liquid filled microtubes." *Experiments in Fluids* 36: 741–747.

Snyder, L. R. and H. J. Adler (1976a). "Dispersion in Segmented Flow through Glass tubing in Continuous-Flow Analysis: The Ideal Model." *Analytical Chemistry* 48(7): 1017–1022.

Snyder, L. R. and H. J. Adler (1976b). "Dispersion in Segmented Flow through Glass tubing in Continuous-Flow Analysis: The Nonideal Model." *Analytical Chemistry* 48(7): 1022–1027.

Steijn, V. v., M. T. Kreutzer and C. R. Kleijn (2007). "m-PIV study of segmented flow in microfluidic T-junctions." *Chemical Engineering Science* 62: 7505–7514.

Stroock, A. D., S. K. W. Dertinger, A. Ajdari, I. Mezic, H. A. Stone and G. M. Whitesides (2002). "Chaotic mixers for microchannels." *Science* 295: 647–651.

Suo, M. and P. Griffith (1964). "Two-phase flow in capillary tubes." *Journal of Basic Engineering* 86: 576–582.

Suresh, V. and J. B. Grotberg (2005). "The effect of gravity on liquid plug propagation in a two-dimensional channel." *Physics of Fluids* 17: 031507–1–031507–15.

Sussman, M., P. Smereka and S. Osher (1994). "A Level set approach for computing solutions to incompressible two-phase flow." *Journal of Computational Physics* 114(1): 146–159.

Suzuki, A. and D. M. Eckmann (2003). "Embolism bubble adhesion force in excised perfused microvessels." *Anesthesiology* 99: 400–408.

Swift, M. R., W. R. Osborn and J. M. Yeomans (1995). "Lattice Boltzmann Simulation of Nonideal Fluids." *Physical Review Letters* 75(5): 830.

Taha, T. and Z. F. Cui (2002). "CFD modelling of gas-sparged ultrafiltration in tubular membranes." *Journal of Membrane Science* 210(1): 13.

Taha, T. and Z. F. Cui (2004). "Hydrodynamics of slug flow inside capillaries." *Chemical Engineering Science* 59(6): 1181–1190.

Taha, T. and Z. F. Cui (2006). "CFD modelling of slug flow inside square capillaries." *Chemical Engineering Science* 61(2): 665.

Taylor, G. I. (1961). "Deposition of a viscous fluid on the wall of a tube." *Journal of Fluid Mechanics* 10: 161–165.

Thomas, S., A. Esmaeeli and G. Tryggvason (2010). "Multiscale computations of thin films in multiphase flows." *International Journal of Multiphase Flow* 36: 71–77.

Thompson, P. A. and S. M. Troian (1997). "A general boundary condition for liquid flow at solid surfaces." *Nature* 389: 360–362.

Thulasidas, T. C., M. A. Abraham and R. L. Cerro (1995). "Bubble-train flow in capillaries of circular and square cross section." *Chemical Engineering Science* 50(2): 183–199.

Thulasidas, T. C., M. A. Abraham and R. L. Cerro (1997). "Flow patterns in liquid slugs during bubble-train flow inside capillaries." *Chemical Engineering Science* 52(17): 2947.

Trachsel, F., A. Gunther, S. A. Khan and K. F. Jensen (2005). "Measurement of residence time distribution in microfluidic systems." *Chemical Engineering Science* 60: 5729–5737.

Triplett, K. A., S. M. Ghiaasiaan, S. I. Abdel-Khalik, A. LeMouel and B. N. McCord (1999b). "Gas-liquid two-phase flow in microchannels: Part 2: void fraction and pressure drop." *International Journal of Multiphase Flow* 25(3): 395–410.

Triplett, K. A., S. M. Ghiaasiaan, S. I. Abdel-Khalik and D. L. Sadowski (1999a). "Gas-liquid two-phase flow in microchannels Part 1: two-phase flow patterns." *International Journal of Multiphase Flow* 25(3): 377–394.

Tryggvason, G., M. Sussman and M. Y. Hussaini (2007). Immersed boundary methods for fluid interfaces. *Computational methods for multiphase flow*. A. Prosperetti and G. Tryggvason, Cambridge University Press**:** 37–77.

Tsai, T. M. and M. J. Miksis (1994). "Dynamics of a drop in a constricted capillary tube." *Journal of Fluid Mechanics* 274: 197–217.

Ubbink, O. and R. I. Issa (1999). "A method for capturing sharp fluid interfaces on arbitrary meshes." *Journal of*

Computational Physics 153(1): 26.

Unverdi, S. O. and G. Tryggvason (1992). "A front-tracking method for viscous, incompressible, multi-fluid flows." *Journal of Computational Physics* 100(1): 25.

van Baten, J. M. and R. Krishna (2004). "CFD simulations of mass transfer from Taylor bubbles rising in circular capillaries." *Chemical Engineering Science* 59(12): 2535–2545.

van Baten, J. M. and R. Krishna (2005). "CFD simulations of wall mass transfer for Taylor flow in circular capillaries." *Chemical Engineering Science* 60(4): 1117–1126.

Walsh, E. J., Y. S. Muzychka, P. A. Walsh, V. Egan and J. Punch (2009). "Pressure drop in two phase slug/bubble flows in mini scale capillaries." *International Journal of Multiphase Flow* 35: 879–884.

Walsh, P. A., E. J. Walsh and Y. S. Muzychka (2009). Laminar slug flow- heat transfer charachteristics with a constant heat flux boundary. *ASME Summer Heat Transfer Meeting*. San Francisco, CA**:** 1–10.

Wang, S. and D. Liu (2008). "Hydrodynamics of Taylor flow in noncircular capillaries." *Chemical Engineering and Processing: Process Intensification* 47: 2098 –2106.

Warnier, M. J. F., E. V. Rebrov, M. H. J. M. de Croon, V. Hessel and J. C. Schouten (2008). "Gas hold-up and liquid film thickness in Taylor flow in rectangular microchannels." *Chemical Engineering Journal* 135(Supplement 1): S153 –S158.

White, F. M. (1991). *Viscous Fluid Flow*, McGraw-Hill.

Yang, C. Y. and C. C. Shieh (2001). "Flow pattern of air-water and two-phase R-134a in small circular tubes." *International Journal of Multiphase Flow* 27(7): 1163.

Yang, Z. L., B. Palm and B. R. Sehgal (2002). "Numerical simulation of bubbly two-phase flow in a narrow channel." *International Journal of Heat and Mass Transfer* 45(3): 631.

Youngs, D. L. (1982). Time-dependent multi-material flow with large fluid distortion. *Numerical Methods for Fluid Dynamics*. K. W. Morton and M. J. Baines. New York, Academic**:** 273–285.

Yu, Z., O. Hemminger and L.-S. Fan (2007). "Experiment and lattice Boltzmann simulation of two-phase gas-liquid flows in microchannels." *Chemical Engineering Science* 62(24): 7172.

Yue, J., L. Luo, Y. Gonthier, G. Chen and Q. Yuan (2009). "An experimental study of air-water Taylor flow and mass transfer inside square microchannels." *Chemical Engineering Science* 64(16): 3697–3708.

Zhao, T. S. and Q. C. Bi (2001). "Co-current air-water two-phase flow patterns in vertical triangular microchannels." *International Journal of Multiphase Flow* 27(5): 765.

Zhao, T. S. and Q. C. Bi (2001a). "Co-current air-water two-phase flow patterns in vertical triangular microchannels." *International Journal of Multiphase Flow* 27(5): 765–782.

Zhao, T. S. and Q. C. Bi (2001b). "Pressure drop characteristics of gas-liquid two-phase flow in vertical miniature triangular channels." *International Journal of Heat and Mass Transfer* 44(13): 2523–2534.

Zheng, Y., H. Fujioka and J. B. Grotberg (2007). "Effects of gravity, inertia and surfactant on steady plug propagation in a two-dimensional channel." *Physics of Fluids* 19: 082107–1–082107–16.